Eur. Phys. J. B **6**, 425–445 (1998)

THE EUROPEAN PHYSICAL JOURNAL B

Atomic self-diffusion in dodecagonal quasicrystals*

J. Roth[1,a] and F. Gähler[1,2,b]

[1] Institut für Theoretische und Angewandte Physik, Universität Stuttgart, Pfaffenwaldring 57, 70550 Stuttgart, Germany
[2] Centre de Physique Théorique, École Polytechnique, 91128 Palaiseau, France

Received: 11 March 1998 / Received in final form and Accepted: 30 July 1998

Abstract. A molecular dynamics study of atomic self-diffusion in Frank-Kasper type dodecagonal quasicrystals is presented. It is found that the quasicrystal-specific flip mechanism for atomic diffusion, predicted by Kalugin and Katz, indeed occurs in this system. However, in order to be effective, this mechanism needs to be catalyzed by other defects, such as half-vacancies. For this reason, it is difficult to distinguish from standard vacancy diffusion.

PACS. 61.44.Br Quasicrystals – 66.30.-h Diffusion in solids – 61.72.Ji Point defects (vacancies, interstitials, color center, etc.) and defect clusters

1 Introduction

Atomic diffusion in quasicrystals has become a topic of considerable interest recently. Stimulated by a paper of Kalugin and Katz [1], in which a diffusion mechanism specific to quasicrystals was proposed, several Monte-Carlo studies for random tiling models have been carried out by a number of groups [2–7]. These studies show that the quasicrystal-specific *flip moves* indeed can add up to global diffusion. From these simple tiling models it is not possible, however, to reliably estimate the size of this quasicrystal-specific diffusion component, nor of its activation energy. In fact, it is even not clear *a priori* whether the elementary flips proposed by Kalugin and Katz [1] are energetically feasible processes. To decide this question, and to be able to better compare with the recently obtained experimental results [8–16], we have carried out molecular dynamics (MD) simulation on a realistic quasicrystal model.

The elementary processes in the *flip mechanism* consist of certain quasicrystal-specific rearrangements of atoms, where the initial and final configurations are energetically almost degenerate. In quasicrystals which are decorations of quasiperiodic tilings with atoms, the flip mechanism consists of a reshuffling of certain local tile configurations, along with their decorations. One goal of our MD simulations was to check the feasibility of the flip mechanism. For such a simulation, not only a realistic model structure is needed, but also (short range) interatomic potentials stabilizing the model structure. Fortunately, this has become available: Dzugutov [17] has discovered a one-component system stabilized by a simple potential in an MD simulation. The supercooled liquid solidifies into a quasicrystalline structure already known as a realistic model of dodecagonal quasicrystals [18,19]. Our models, perfect and defective versions of this structure, are layered structures essentially of Frank-Kasper type. They are periodic in one direction.

We find that the flip mechanism [20] indeed occurs, but, since the structure is mostly close-packed and thus very rigid, this process has a very high activation energy. However, it can efficiently be catalyzed by the presence of other defects, such as vacancies and half-vacancies. The latter are associated with the breaking of periodicity in the third direction. Unfortunately, the effects of vacancy diffusion and flip diffusion are hard to separate. While the presence of vacancies and half-vacancies is required for the flip mechanism to work, these same vacancies, of which there is always an equilibrium density of about 2.5% present in our simulations, also lead to ordinary vacancy diffusion, which can mask the flip diffusion.

The paper is organized as follows: In Section 2 we discuss the dodecagonal quasicrystal model and its geometrical and topological properties. Section 3 is devoted to an introduction of the interaction, simulation method, and analysis tools. In Section 4 we present the results of our simulations and finish with the conclusions in Section 5.

2 The dodecagonal model quasicrystal

2.1 Structure features of the ideal tilings

The structure model of the dodecagonal quasicrystal is a layered system which, apart from some defects, is periodic

* This work is dedicated to Prof. Hans-Ude Nissen on the occasion of his 65th birthday.

[a] e-mail: johannes@itap.physik.uni-stuttgart.de
[b] e-mail: gaehler@itap.physik.uni-stuttgart.de

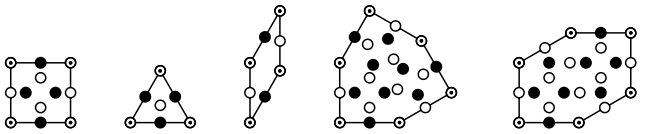

Fig. 1. The basic tiles of the dodecagonal model: square, triangle, rhombus, shield, twofold symmetric hexagon. The dotted atoms are placed in A-layers $z = 1/4$ and $3/4$, the white atoms in B-layers at $z = 0$, and the black atoms in $\bar{B}$-layers at $z = 1/2$. All tiles can also occur with black and white atoms exchanged, depending on their orientation. The twofold symmetric hexagon is unstable and does not occur in our tilings.

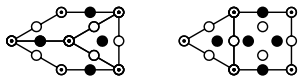

Fig. 2. Transformation from a rhombus pair and a triangle to a triangle and a square.

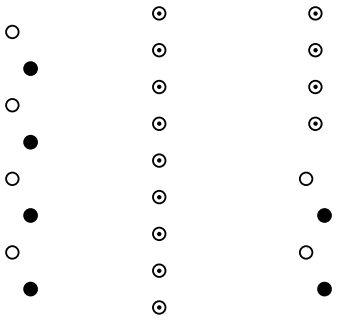

Fig. 3. Different configurations of a column: staggered (left), vertical (middle), and half staggered/half vertical, with a half-vacancy in between (right).

in one direction, but quasiperiodic and 12-fold symmetric in the plane perpendicular to it. It basically is of Frank-Kasper type, *i.e.*, it is mostly tetrahedrally close-packed, and can be described as a periodic stacking $AB A\bar{B}$ of a primary dodecagonal layer A and two secondary hexagonal layers, B and $\bar{B}$, which are rotated by 30° with respect to each other, to obtain dodecagonal symmetry. The atoms in layer A form the vertices of a simple tiling made of squares, triangles, 30° rhombi and two kinds of hexagons. These tiles, together with their decorations, are shown in Figure 1. The dodecagonal quasicrystal structure can therefore be regarded as a decoration of a simple dodecagonal tiling [18,19]. It is an excellent model for dodecagonal Ni-Cr quasicrystals [21], but is also related to the structure of dodecagonal Ta-Te and its approximants [22]. The squares and triangles can also be assembled to a number of well-known crystalline phases (Sect. 2.3), which are closely related to dodecagonal quasicrystals.

All structures based on a tiling with squares and triangles only are perfectly tetrahedrally close-packed. Such structures are therefore very rigid, and there are only few small groups of tiles that can be reshuffled [23]. If hexagons or rhombi are present, however, some atoms do not have a close-packed environment. Octahedral neighbourhoods occur in the interior of hexagons and at the obtuse corners

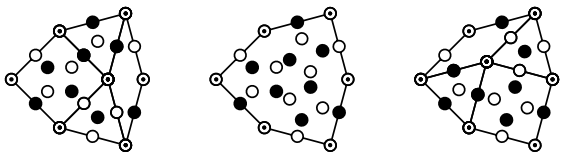

Fig. 4. Rotatory flip of the shield with one rhombus. The three parts show local minima.

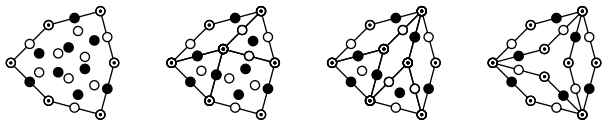

Fig. 5. The possible configurations inside the shield. The first two configurations are stable. The third one relaxes quickly into one of the first two, if present in the initial configuration. The last arrangement is very unstable and is not found in our simulations.

of the rhombi. Near the octahedra, the structure is much softer than on average. All structures with the same area and height contain the same number of atoms, since all structures can be transformed by shifts of atoms into an square-triangle-tiling. The density in all structures with the same volume is thus identical.

In the structures containing hexagons and rhombi there are many local tile configurations which can easily be reshuffled. This is achieved by small shifts of some atoms from A layers into the B and $\bar{B}$ layers, or *vice versa*. These reversible shifts shall be called "flips" in the following. As the first such flip we discuss the transformation of a pair of rhombi and a triangle into a square and a triangle (or *vice versa*), as shown in Figure 2. In this process, only one (straight) column of atoms in A layers has to be changed into one (staggered) column of atoms in B- and $\bar{B}$-layers (Fig. 3). This is achieved if all atoms in the column make a little move diagonally upwards (or downwards), with alternating directions in the quasiperiodic plane. The same column move and its inverse also trigger all the other flip processes. Particularly important is the flip which replaces the interior of a hexagon containing a square, two triangles and a rhombus by a perfectly three-fold symmetric configuration called *shield* (Fig. 4), or *vice versa*. By two consecutive such flips, a rhombus can change its position within the hexagon (Fig. 4). In fact, by consecutive column moves any of the four possible shield-shaped configurations (Fig. 5) in any orientation can be transformed into any other. Similarly, the three configurations filling a flat hexagon (Fig. 6) can be transformed into each other by column moves. A sequence of two such flips allows a rhombus to change its position (Fig. 7). A further important flip is the one shown in Figure 8, where a shield changes its position. This large jump of the shield is triggered by only two nearby column moves. All flip processes can be broken down to the elementary processes described above, and these in turn can be decomposed into individual column moves.

In a perfect structure the column moves are not very easy, however. In such a move all atoms in a whole column

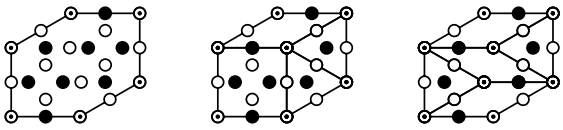

Fig. 6. The possible configurations inside the two-fold symmetric hexagon. The fist configuration is stable, while the second may occur slightly destorted as a transition state. The last arrangement is unstable and relaxes immediately, if present at the beginning of a simulation.

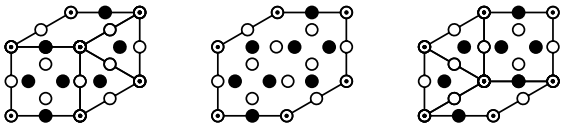

Fig. 7. Translational flip of the twofold symmetric hexagon. The central configuration is not exactly the saddle point, since the flipping atoms are shifted by 1/10 of the period along the periodic axis.

have to move upwards or downwards, whereas other atoms change their position very little. Such a process seems not very likely, since the vertical distance of atoms is already rather small, which means that there is no place for an atom to start moving. Only at places where the structure is not perfectly close-packed the atoms can find some space to move sideways. In this way, a column move can be started, and flips are indeed possible, as our results will show (see Sect. 4).

Although the structure is mostly close-packed and therefore very dense, there exist characteristic anisotropies in the model, which result in a anisotropic mobility of the atoms along the periodic axis. Along this axis, the atoms are arranged in straight closed-packed columns, which allow collective moves of the atoms. In the quasiperiodic plane and in oblique directions there are *no* such close-packed rows, which would allow collective moves of the atoms over a longer distance.

2.2 Point-like defects

In the presence of vacancies, the column moves and thus the flip processes become much easier. Since between two atom positions in a column parallel to the periodic axis there is another good atom position, a neighboring atom of a vacancy can move half-way into the vacancy, effectively splitting it into two half-vacancies, which can then move up and down the column independently, and transform it from the vertical configuration into the staggered configuration and vice versa (Fig. 3). Such half-vacancies therefore efficiently catalyze the various flip moves introduced above. The half-vacancies are also responsible for a possible breaking of the periodicity in z-direction.

Half-vacancies are larger than octahedral holes, but smaller than vacancies at ordinary atomic sites. They do not occur in structures which are stacked perfectly periodically. Due to the close-packed nature, there are only tetrahedral holes, and octahedral holes at the centers of

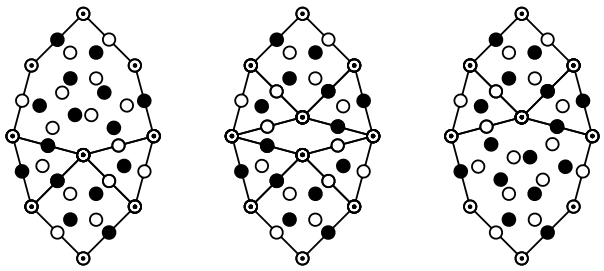

Fig. 8. Translational flip of the shield. The three parts show local minima.

the shields and the obtuse corners of the rhombi, where the structure is not close-packed. Half-vacancies occur at places where strict periodity is broken. Typical examples of such places are a triangle-rhombi configuration stacked onto a square-triangle configuration (Fig. 2), and a shield stacked onto a shield-shaped hexagon filled with a rhombus, two triangles and a square (Fig. 4). Half-vacancies always occur when the staggered column configuration with atoms in the B and $\bar{B}$ layers switches to a vertically stacked configuration with atoms in the A layers (Fig. 3).

As a complement to the half-vacancies there are also places where atoms are too close together, forming sort of a half-interstitial. This arrangement is completely unstable, however, due to the hard core repulsion of the atoms. The neighbouring atoms are shifted by a small amount, until all the atoms have a proper distance from each other. This process causes some local distortion of the structure.

The high packing density has a further effect: the tilings in all the layers are forced to be identical, as long as the structure is in equilibrium and the potential energy is optimal. If we take two adjacent A layers, we find that the B atoms are located exactly in the bumps of these layers, which imposes a strong coupling, so that there is no freedom for the tiling to change from one A-layer to the next. Stacking faults therefore are possible only at a considerable energy cost.

2.3 Samples used in the simulation

For the simulations we have constructed samples based on several tilings of different sizes and with different types of tiles. Dodecagonal tilings can be formed in a variety of ways using squares, triangles, rhombi and hexagons. The samples used in our simulations are based on four different types of such tilings: with squares and triangles only (SqTr), with additional shields (Shi) or with additional rhombi (Rho), and random tilings made of squares, triangles and rhombi (Ran). The Ran samples also contain rhombi adjacent to each other, which is not the case for the Rho samples. Furthermore, we have used a small tiling called Dod, which consists of a regular dodecagon (filled with triangles and squares) plus one square and four triangles.

Most samples are built as a periodic stacking of layers based on the same tiling. In addition we have also

Table 1. Number of tiles per period and total number of A atoms for the tilings used in the simulations. Tiles types: S: squares, T: triangles, R: rhombi, H: shields. The names for the tilings are given in the text. I and F: number of atoms in the A layer at the beginning and at the end of the simulation, respectively. For the three groups of structures, a single period contains 112, 836 and 4680 atoms, respectively, and the simulation cells consisted of 2, 10 and 3 periods.

name	S	T	R	H	I	F
Dod2	4	12	0	2	56	56-64
SqTr	52	120	0	0	2240	2240
Rho/Ran	44	120	16	0	2400	–
Shi	28	88	0	16	2040	2040
SqTrFlat	291	672	0	0	3762	3762
AperFlat	246	672	90	0	4032	3670
ShiFlat	156	492	0	0	3492	3620

used samples obtained by stacking layers based on *different* tilings. We call this a random stacking, although the sequences are chosen so that the mismatches between neighbouring layers are minimal. There are a few short distances due to the mismatches, but they can be removed by carefully relaxing the starting configuration. No changes in the atomic positions between the originally prepared and then relaxed configurations beyond local adjustments have been observed.

The aperiodicity of quasicrystals causes a problem with the boundary conditions in the simulation. Taking a finite patch with open boundary conditions should be avoided, because of the large surface effects which affect the stability of the structure. The solution is to use periodic approximants, which are finite, rectangular bricks whose borders fit together on opposite sides. In this way, periodic boundary conditions can be used, which is done throughout this paper.

Simulation cells of three different sizes have been used. The first cell is approximately cubic. The samples with this cell shall be called the "cubic" ones. In the quasiperiodic plane this cell has an edge length of $5 + 3\sqrt{3} = (2 + \sqrt{3}) * (1 + \sqrt{3})$ tile edges. Along the z-axis the cell contains 10 basic $AB\bar{A}\bar{B}$ layers, which are decorations of either the SqTr, the Shi, the Rho or the Ran tiling. The resulting samples are denoted by the same names. In addition, we have also used a cubic sample obtained from a random stacking of different tilings. This sample is called Aper. Independently of the underlying tiling, the cubic samples all contain 8360 atoms each.

The second simulation cell contains only three basic $AB\bar{A}\bar{B}$ layers, but has an edge length of $12 + 7\sqrt{3} = (2 + \sqrt{3})^2 * \sqrt{3}$ in the quasiperiodic plane. These samples, which shall be called the "flat" ones, are built on either the SqTr or the Shi tiling, or with a random stacking of different tilings. These samples are called SqTrFlat, ShiFlat and AperFlat, respectively, and contain 14040 atoms each.

Finally, we have used samples based on the Dod tiling, whose edge length is $2+\sqrt{3}$. These samples have a varying number of layers. Up to 15 layers have been used, in order to study the influence of size of the simulation box in the periodic direction. Details of the tilings can be found in Table 1.

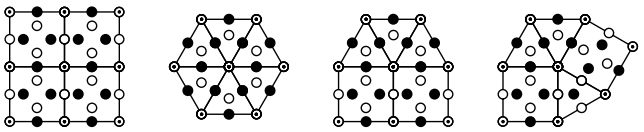

Fig. 9. Crystalline phases with squares and triangles only and a single vertex configuration. From left to right: A15, Z, H and σ phase

In addition to the quasicrystalline tilings, it is also possible to generate crystalline phases with squares and triangles decorated in the same way as in the quasicrystals. If only squares are used, the A15 or β-tungsten structure is obtained, whereas a pure triangle tiling results in the Zr_3Al_4 or Z structure. If both squares and triangles are used, one can obtain the σ-phase (two non-adjacent squares and four triangles per unit cell) or the H-phase (two adjacent squares and four triangles per unit cell). For the crystalline phases we have used samples of a size similar to the "cubic" quasicrystalline samples. The vertex configurations of the crystalline phase are shown in Figure 9.

Up to 2.5% vacancies have been artificially created in the (cubic) SqTr and Shi samples. This is similar to the number of vacancies found by Dzugutov [24] in his simulations. The vacancies in the SqTr sample have been created at tiling vertices, at tile edge centers, or in the interior of the triangle or a square. The resulting samples are called SqTr_vert, SqTr_edge, SqTr_tri and SqTr_sq, respectively. A sample with vacancies on arbitrarily chosen locations is called SqTr_any. In a similar way, vacancies have been introduced in the Shi sample, at sites inside the shield. There are two kinds of such sites. Those near the rectangular corners are analogous to the sites inside a square. Samples with such vacancies are called Shi_sq. The remaining six sites inside a shield form an octahedron. Near these sites the structure is not tetrahedrally close-packed. Samples with vacancies at such sites are called Shi_oct. There are also samples with fewer vacancies, in which case we indicate their concentration (1.3%).

3 Setup for the simulations

3.1 Interaction

For our simulations we used a potential similar to the one described by Dzugutov [25]. The special feature of Dzugutov's potential is that it has a minimum at 1.13σ [1] of depth -0.581ϵ similar to the well-known Lennard-Jones

[1] All physical properties in this paper are given in standard Lennard-Jones units ϵ and σ [26], where $-\epsilon$ is the depth of the potential minimum and σ the distance of two atoms at the radius of the potential minimum. Quantities given in reduced units are indicated by a $*$.

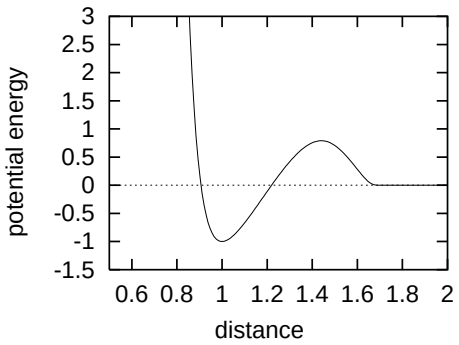

Fig. 10. The Dzugutov potential used in this paper.

potential, but also has a maximum at 1.63σ of height 0.460ϵ, and then goes to zero continuously. The maximum is designed to prevent the system from crystallizing into simple crystal phases like fcc, hcp or bcc. The potential has a short finite range of $r_c = 1.94\sigma$, which is important to keep the computation time within reasonable limits. In our simulations we have used a rescaled version of Dzugutov's potential, so that its minimum is exactly at $-\epsilon$. To compare Dzugutov's results with ours one has to rescale the energies accordingly. Especially our temperature scale has to be multiplied by 0.581 to get into agreement with Dzugutov's data. The potential is displayed in Figure 10. In the simulations we have tabulated the potential for too reasons: this makes it easier to change from one potential to another, and it improves the performance of the simulation program if the potential is defined by a complicated function.

3.2 Simulation method

The equilibrium molecular dynamics simulation method was applied to determine the equilibrium shape of the simulation box and to explore the pressure-temperature phase diagram of the system. This procedure requires a constant-pressure-constant-temperature ensemble (NPT) instead of the standard microcanonical constant-volume-constant-energy ensemble (NVE). To implement the NPT ensemble we use the constraint method of [27]. The equations of motion are modified by terms rescaling the simulation box size and accelerating or slowing down the atoms. Since we have a layered structure, with a simulation box which has only tetragonal instead of cubic symmetry, it is appropriate to allow the three box dimensions to fluctuate independently. This is possible with the simulation scheme introduced in [28].

The equations of motion are integrated by a fourth-order Gear predictor-corrector algorithm (see, for example, [26]). The predictor-corrector algorithm allows us to trace the trajectories of the atoms more accurately than with the simpler Verlet schemes, and up to recently it was not known how to implement Verlet-like integration methods in the case of modified equations of motion.

The time increment of the integration steps δt^* was adjusted after testing for numerical stability. We find that $\delta t^* = 0.005$ is an appropriate value. For simplicity, and since there is only one type of atoms, the masses of all atoms where set to unity. Depending on the results, the simulations took from as few as 10,000 up to as many as 3×10^7 time steps, after an additional equilibration period of 10,000 steps.

3.3 Physical accuracy of the diffusion measurements

Changing the thermodynamic ensemble from the standard microcanonical NVE ensemble to another ensemble always changes the trajectories of the atoms. All methods used for simulations of ensembles where pressure or temperature or both are fixed have to change the equations of motion, and therefore affect the ordinary velocities and positions of the atoms. The constraint method changes the trajectories in the least possible way, since it is a realization of the Gaussian principle of the least constraint. The trajectories of the atoms therefore do not represent the physical ones found in microcanonical ensemble simulations. It should be kept in mind, however, that any single trajectory computed in any ensemble depends in any case on many non-physical things, in particular the computer precision. A single trajectory therefore should not be overinterpreted. It is rather the statistics over many trajectories which does have a physical meaning. In a simulation one may, for example, calculate the mean square displacement and derive the diffusion constant from it. We find that such averages are independent of the simulation ensemble that is chosen, if they are evaluated properly.

3.4 Applicability of molecular dynamics simulations

A serious limitation of molecular dynamics simulations is the characteristic time scale of the processes we are interested in. If this time scale is of the order of the simulation time or longer, it is not possible to get equilibrium results. This is the case for diffusion simulations. Most of the time the atoms are only fluctuating around their equilibrium position. The typical time scale of the fluctuations and of atomic jumps is about 10^{-13} s [29]. To represent the motion of the atoms accurately, the simulation requires time increments of the order of 10^{-15} s. The typical residence time of an atom in a metal just below the melting point is 10^{-7} s, which is a factor of a million longer than a jump process. It would thus take 10^8 steps to see a single atom jump once. But since we have of the order of 10,000 atoms, we can expect a total of about 100 jumps during a typical simulation with one million time steps. For these reasons it is in general not possible to calculate the diffusion constant accurately as a function of temperature, especially at low temperatures where jumps are even less frequent.

There are other limitations for computer simulations, resulting from the limited size of the sample. By applying periodic boundary conditions to avoid surface effects, the diffusion behaviour may be changed. To create vacancies, atoms have to move to the surface, which is no longer possible with periodic boundary conditions.

The only way to create vacancies is to remove atoms from the sample, but to do this correctly the equilibrium density of vacancies has to be known and, what is more important, the relevant diffusion mechanisms must be known beforehand.

Molecular dynamics is a good tool, however, to find the types of jumps that occur and to extract the basic jump paths. It is then possible to calculate the diffusion barriers, the activation energies and the jump frequencies. These results may be used in Monte-Carlo simulations, where the simulation steps are no longer limited to the vibrations of the atoms around their equilibrium position, but are the basic jump processes. In this way, it is possible to derive the actual diffusion constants and the long-time diffusion behaviour.

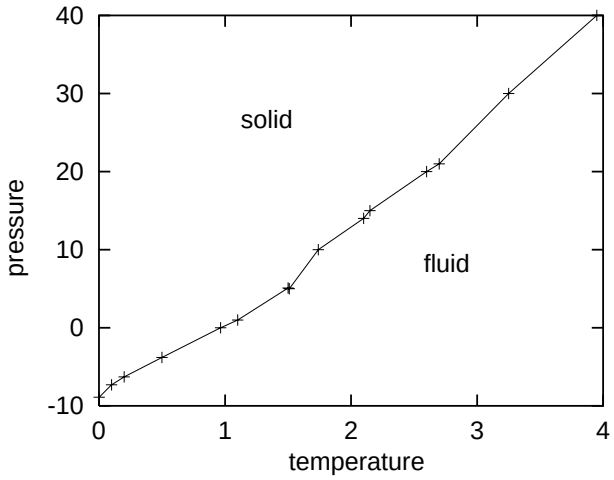

Fig. 11. Pressure-temperature phase diagram for the Dzugutov potential. This is not a phase diagram of thermodynamic equilibrium, but the transition line indicates where the sublimation occurs in a heating simulation experiment.

3.5 Phase diagram

The ground state structure of Dzugutov's potential is not known with certainty [30]. Since it is not possible to explore the whole configuration space for densely packed solid structures by standard computer simulation methods, the only thing one can do is to run simulations for different plausible structures, and to compare their thermodynamical properties. We have done this comparison for the structures described in Section 2, as well as for some simple crystalline phases. These simulations indicate that the ground state of the Dzugutov potential is not the quasicrystal or one of its approximating crystalline phases described in Section 2, but rather a simple bcc crystal [30]. Apart from this bcc phase, the crystalline σ phase turns out to be the most stable phase. It consists of the same triangles and squares as the quasicrystalline SqTr phase, which we have used to determine the part of the pressure-temperature phase diagram where the square-triangle structures are solid and meta-stable[2]. A series of simulations was run at fixed temperature and pressure, starting with the solid structure. Beginning at low temperatures, we increased the temperature until the sample underwent a phase transition. Further simulations between the last point in the solid range and the first point in the liquid range where used to pin down the transition line with more accuracy. This procedure was carried out for a number of pressure values to get the full transition line presented in Figure 11.

The system does not melt at the phase transition at $T^* = 0.95$ and $P^* = 0.001$, but rather sublimates. For Dzugutov's structure we find a different melting temperature ($T^* = 0.7$), due to defects in the structure. After the transition the potential energy is close to zero, which means that the coordination number is very low and the atoms are nearly unbound. The volume increases by a large factor, which further indicates that the new phase is a gas. We have performed a number of simulations along the phase transition line with increasing temperatures to find a triple point, but without success. The difference in potential energy between the solid and fluid phase diminishes and becomes too small to be resolved by molecular dynamics at $T^* = 2$ and P^*=15. We have to point out, however, that a more thorough investigation of the phase diagram would require a calculation of the Gibbsian free energy. This has not been carried out, since it is beyond the topic of this study.

The long-time diffusion simulations were run at $T^* = 0.6$, which is rather close to the melting temperature $T^*_m = 0.95$. The high temperature was necessary to keep the atoms sufficiently mobile. The hydrostatic pressure applied in all simulations was $P^* = 0.001$.

3.6 Analysis tools

To analyze the equilibrium structures in detail, we quenched the configurations to zero temperature by setting the temperature in our NPT-MD-program to $T^* = 0$ and $\delta t^* = 0.0001$, thereby using the program as a steepest descent algorithm. The quenching has the effect that all the atoms move to the local energy minimum. To check the validity of this procedure, we compared the *in situ* and the quenched structures, and found that there are no substantial differences. The next step is to calculate the Voronoi cells and their dual Delaunay cells, and to determine from the latter the distribution of the hole sizes (free volumes) in the structure (see Fig. 12). The diagram indicates that there are vacancies in Dzugutov's structure obtained by cooling. The density of the vacancies is about 2.5%.

Although the distribution of free volumes gives a reasonable representation of the small interstitial sites, it largely overestimates the vacancies by a factor of about ten. This happens because the Delaunay cells are face-to-face packed tetrahedra, whereas the vacancies should

[2] The situation is similar to the Lennard-Jones case. Usually one simulates fcc structures, although the ground state is hcp.

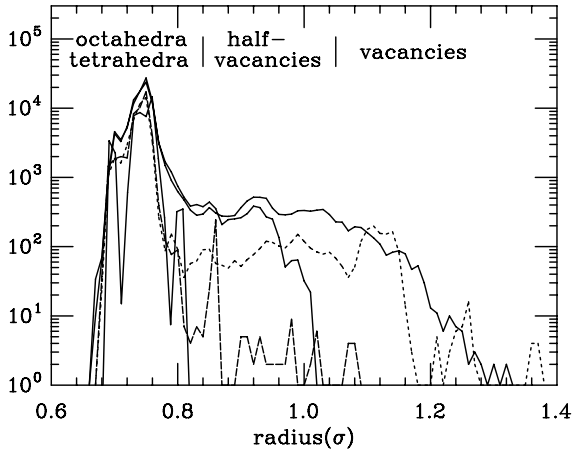

Fig. 12. Histogram of hole sizes for different structures, after cooling to zero temperature. There are holes inside tetrahedra, holes inside octahedra, half-vacancies, and full vacancies, where entire atoms fit in. The data of Dzugutov's structure is shown in solid, both before and after the full vacancies have been filled. The data for a square-triangle-shield structure is shown dashed, after a very long simulation, both with (short dashed, Shi_oct) and without (long dashed, Shi) initial holes.

be represented by spheres which can easily cover several tetrahedra. To solve this problem, we filled all the vacancies with spheres. We start at a certain Delaunay cell and create a tree connecting all Delaunay cells with a center distance to the first cell smaller than the minimal atom distance. We repeat this procedure until the tree includes all Delaunay cells that would contain mutually overlapping spheres. Then we fill the tree with spheres, starting at the outmost ends. After adding a sphere, all the Delaunay cells covered by it are discarded. Then the next sphere is added on the next outermost Delaunay cell left, and so on. This procedure is repeated until the whole tree is filled. Then the algorithm starts again with a Delaunay cell not yet visited. This method allows us to fill the sample as densely as possible with vacancy atoms.

3.7 Characteristic lengths

One of the useful properties of the square-triangle-rhombi-shield model is that it is possible to reconstruct the whole tiling from the atomic positions only. This is especially valuable in molecular dynamics simulations. The basic length is the edge of a tile. In the simulation it is the average distance of two neighboring atoms in the same primary A layers. Connecting all the atoms with this separation reconstructs the underlying the tiling. Other characteristic lengths may be easily found from geometrical considerations. Specific tiles like the rhombi can be found by searching for atoms with their short diagonal distance, shields are found by looking for all triangles with an edge length of the diagonal of the square containing no further atom in the A layer.

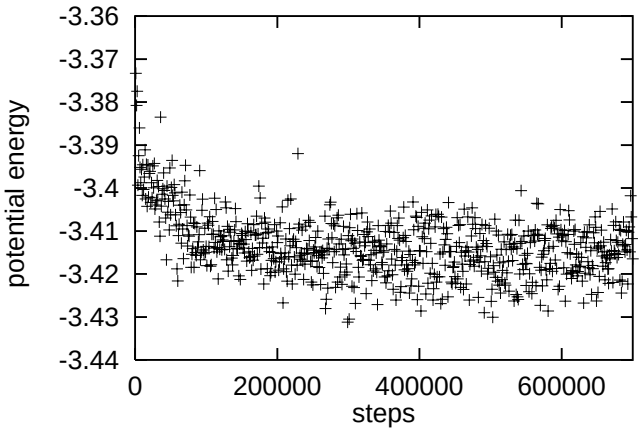

Fig. 13. Relaxation of the potential energy (AperFlat sample).

4 Results

We first present the results that are valid for all samples, irrespectively of whether they are perfect, have defects, instable vertex configurations or stacking disorder. Then we proceed with the results for structures without vacancies (but including structures with stacking disorder), first for the samples with many layers, and then for the flat samples. Finally, the results for the structures with vacancies are presented, again first for the samples with many layers, then for the flat samples. In each case, the potential energy, the mean square displacement of the atoms, the atomic displacements, and the jumps and the flips of the tiling are determined. The flips observed in the flat samples will be analyzed, and the activation and barrier energies will be calculated.

4.1 General results

In all simulations we have monitored the potential energy during the whole simulation time. After an equilibration period of 10,000 time steps, and also at the end of the simulation, we have quenched the structure from the simulation temperature $T^* = 0.6$ to $T^* = 0$ to get the static equilibrium positions of the atoms. The resulting energies are given in Table 2. We note that there is not much difference between the energies within the groups separated by the horizontal lines, with the following two exceptions. The Ran samples containing pairs of rhombi clearly improve during simulation. The same is true for the random stacking structures, where the initial energies before relaxation were -3.292 and -3.375 for the cubic and the flat sample, respectively. The relaxation process can be observed in Figure 13. It lasts about 300,000 simulation steps. Among the structures studied (and apart from the simple bcc phase), the best structure is the σ-phase, but the dodecagonal square-triangle tiling is very close. The worst is the pure triangle phase, and we will have to deal with the special properties of this phase later. The pure square phase and the H-phase are not so good, either.

Table 2. Potential energies per atom and number of simulation steps. Subscripts: O: orthogonal, C: cubic, I: initial state at $T^* = 0.01$ (SqTrFlat, ShiFlat, and Dod* at $T^* = 0.1$), S: simulation average at $T^* = 0.6$, Q: quenched to $T^* = 0$ after simulation. The names of the phases are explained in the text, 16384 is Dzugutov's sample in an isothermal-isobaric ensemble, NVT the same as an isothermal-isochoric ensemble. In the 16,770 and 16,888 simulation additional atoms have been put into the vacancies. Flat samples contain 14,040 atoms, cubic samples 8360 atoms. The digits after Dod indicate the number of periods. Two energy values are given if the structure relaxes during simulation. "–" means that the value has not been calculated.

phase	V_{OI}	V_{CI}	V_{OS}	V_{CS}	V_{OQ}	V_{CQ}	steps
Aper	−4.367	–	−3.292/−3.408	–	– /−4.395	–	3.00e5
AperFlat	–	–	−3.371/−3.415	–	−4.365/−4.407	–	7.00e5
SqTr	−4.421	−4.419	−3.427	−3.427	−4.420	−4.418	3.43e5
SqTrFlat	−4.244	–	−3.408	–	–	–	1.00e5
Ran	−4.338	−4.338	−3.409	−3.370	−4.405	−4.382	4.47e5
Rho	−4.410	−4.408	−3.370	−3.398	−4.391	−4.390	4.39e5
Shi	−4.391	−4.389	−3.397	−3.400	−4.391	−4.390	3.50e5
ShiFlat	−4.240	–	−3.403	–	–	–	5.00e5
Dod2	−4.245	–	−3.412	–	–	–	300.0e5
Dod3	−4.245	–	−3.405	–	–	–	1.00e5
Dod4	−4.245	–	−3.405	–	–	–	1.00e5
Dod5	−4.245	–	−3.407	–	–	–	20.0e5
Dod6	−4.245	–	−3.410	–	–	–	20.0e5
Dod10	−4.245	–	−3.409	–	–	–	0.14e5
16384	–	−4.097	–	−3.334	–	−4.245	0.10e5
16770	–	−4.240	–	−3.281	–	−4.288	0.10e5
16888	–	−4.228	–	−3.266	–	−4.276	0.10e5
NVT	–	−4.087	–	−3.336	–	−4.248	0.10e5
A15	−4.329	−4.329	−3.365	−3.365	−4.328	−4.328	1.00e5
Z	−4.216	–	−3.177	–	−4.213	–	6.28e5
H	−4.345	–	−3.365	–	−4.345	–	1.00e5
σ	−4.453	–	−3.373	–	−4.453	–	1.50e5
SqTr_any	−4.332	–	−3.341	–	−4.334	–	1.47e5
SqTr_edge	−4.334	–	−3.343	–	−4.336	–	1.47e5
SqTr_vert	−4.336	–	−3.344	–	−4.335	–	2.64e5
SqTr_squa	−4.332	–	−3.339	–	−4.333	–	1.44e5
SqTr_tri	−4.315	–	−3.324	–	−4.315	–	1.48e5
Shi_any	−4.292	–	−3.302	–	−4.303	–	1.54e5
Shi_oct	−4.347	–	−3.357	–	−4.349	–	3.00e5
Shi_oct (1.3%)	−4.366	–	−3.378	–	−4.368	–	3.00e5

This clearly shows that a mixture of squares and triangles is preferable. In Dzugutov's phases and in the samples with vacancies we clearly see the influence of the defects on the potential energy. The length of the simulation runs can also be found in Table 2.

The samples with approximately cubic cell have been simulated with two kinds of periodic boundary conditions. With "orthogonal" boundary conditions the box size is allowed to fluctuate in all three directions independently, whereas with "cubic" boundary conditions only isotropic size fluctuations are permitted. The sample is also slightly distorted to fit into the cubic box. We find that there is not much difference between cubic and orthogonal boundary conditions. Compared to cubic boundary conditions the potential energy is slightly improved with orthogonal boundary conditions, since in the cubic case the layer distance is slightly larger than optimal. With orthogonal boundary conditions the system has more degrees of freedom, which are used to adjust the layer distance with respect to the atom distance in the quasiperiodic plane. The result is a tetragonal box, which reflects the fact that we have used square approximant cells. The pure square phase represents a special case: as mentioned in Section 2.3, this phase is identical to the *cubic* A15 phase.

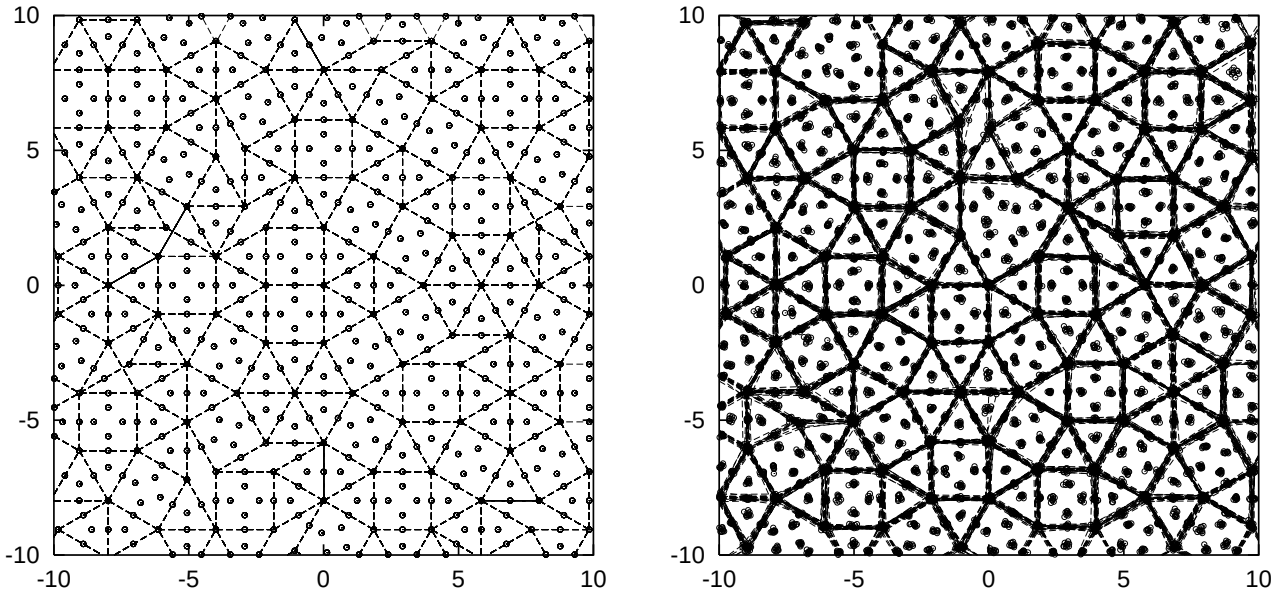

Fig. 14. Comparison of the initial and final configuration after 100,000 simulation steps, for the Ran phase without vacancies. On the left, a projection of the initial state on the xy-plane is shown. On the right, the same structure is shown at the end of the simulation. The tiling has been reshuffled at some places, and at different z-coordinates one has different tilings, so periodicity is slightly broken. Atoms which have moved are primarily inside shields. The tile edges appear as heavy lines because the tilings at different z-levels, all drawn on top of each other, have been reconstructed from the thermally distorted atom positions.

The simulation should therefore prefer a cubic simulation box, which is indeed the case, within the error bounds.

The quotient a/c of the box dimension in the quasiperiodic plane (a) and along the periodic axis (c) is largely independent of the temperature. This means that thermal expansion is approximately isotropic.

4.2 Structures with many layers and without vacancies

Our first goal was to understand the behaviour of the perfect quasiperiodic structures SqTr, Shi, Rho, and Ran, as well as that of the simple crystalline phases, both sets without any defects (vacancies, stacking disorder). Later we will introduce vacancies and start the simulations from randomly stacked samples.

The pure square-triangle tiling structure (SqTr) turns out to be very stable. The same is true for structures containing shields (Shi), and for the crystalline pure square, σ- and H-phase structures. Simulation runs for these phases at $T^* = 0.6$ reveal that no atom changes its place, which means that there are *no* atomic jumps observable, and therefore *no* diffusion and *no* tile flips or relaxation processes occur. In an attempt to facilitate diffusion, the sample had been elongated along the periodic axis to draw the layers apart, but this had no effect on diffusion.

All the other phases studied are stable in the sense that the structure remains a generalized square-triangle-rhombus-shield tiling, and does not change to a crystalline structure, for example. In contrast to the phases discussed before, we observe in the quasicrystalline samples ShiFlat, Rho, Ran, Aper, AperFlat, and in the crystalline pure triangle phase, that atoms can jump, and that even long-range diffusion occurs in a few cases. The tiling may change also by flips and relaxation processes, thereby changing the frequency of certain tiles.

In a more strict sense, the Rho phase containing isolated rhombi should only be called metastable. While it remains unchanged at $T^* = 0$, the rhombi are successively transformed into shields at $T^* = 0.6$, on a time scale of about 300,000 simulation steps. This time is long enough for some of the rhombi to change their places by flipping. The rearrangements yield a short time contribution to the average mean square displacement of the atoms. Since the rearrangement of the tiles is a local process, which can start at different places along the periodic axis at the same time, the final state need not be perfect. A few defects will remain for a longer time, which permits a very low diffusion rate at long time scales. The full periodicity along the z-axis is eventually restored, due to the strong coupling of the layers. The final structure is a square-triangle-shield phase.

The random tiling phase Ran contains in addition some pairs of rhombi. Like the Rho phase it is metastable. At $T^* = 0.6$, the rhombi pairs are even very unstable and recombine immediately, during equilibration already. Since this process is so fast, it can happen that the periodicity is broken for some time, which may trigger jump processes *in the quasiperiodic plane*. Beyond relaxation, the same processes as in the Rho phase occur. In both phases the number of vacancies created is negligible (1 or 2).

Pictures of the changes between the initial and final configurations are presented in Figure 14. Tiles have been drawn to show the flips and the relaxations.

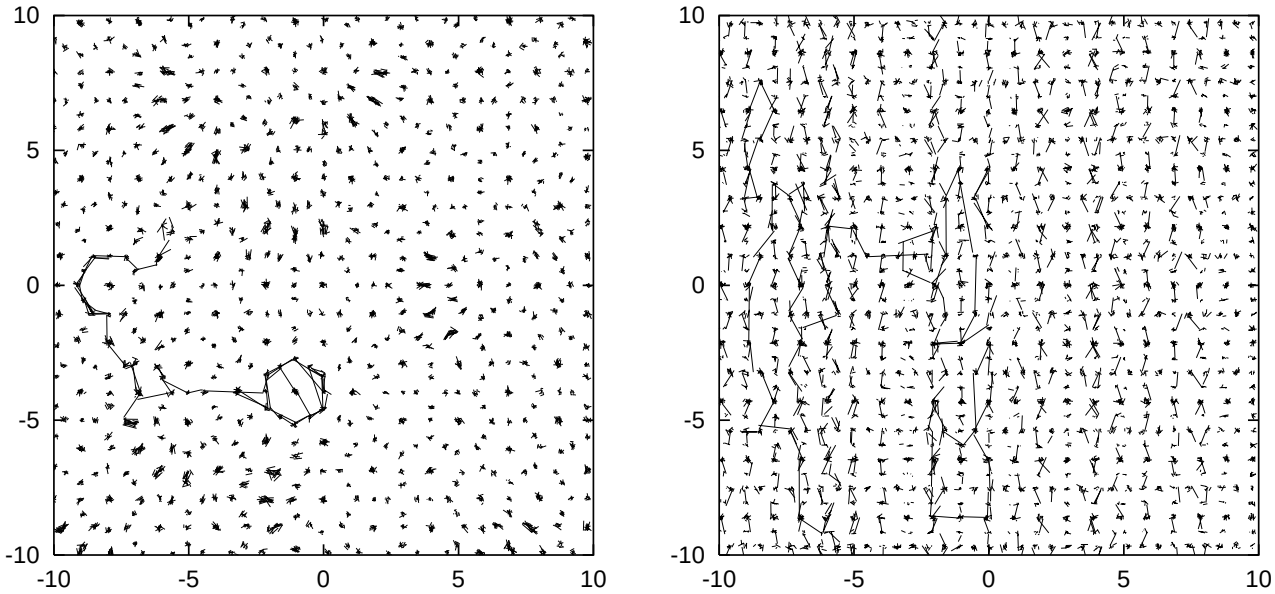

Fig. 15. Comparison of the initial and final configuration after 100,000 simulation steps, for the Ran phase without vacancies. On the left, a projection on the xy-plane is shown, with initial and final positions connected. On the right, a projection of the same structure onto the xz-plane is shown. It can be seen that atoms primarily move vertically, with small horizontal displacements only. Jumps of individual atoms are represented by straight line segments. Zig-zags of several line segments represent chains of atoms which follow each other. If a straight line extends over several layers (right picture), the corresponding atom must have performed several consecutive jumps.

There are some half-vacancies present, which indicate that the periodicity is broken at these places. They are found at obtuse corners of some of the rhombi. The motion of the atoms during the simulation are revealed by Figure 15, where we have connected the initial position of each atom with its final position. In the projection onto the quasiperiodic plane (left picture) one observes on the left side a cascade of atoms which have moved a considerable distance. Longer dashes indicate the relaxations. The projection onto a plane containing the periodic axis (right picture) shows on the right side the relaxation of the rhombi atoms from the A layers to the B and $\bar{B}$ layers. On the left side we find again the fingerprints of the cascade. Note that most of the atoms move only to nearest neighbour places. This will be different if vacancies are present.

The comparison of the initial and final structure reveals the dynamics of the diffusion. It turns out that the atoms jump preferably along the periodic direction. The shifts of the atoms in the quasiperiodic plane are small. In the Rho phase we see consecutive jumps from layer to layer, whereas in the Ran phase only jumps from one layer to the next have been observed. The reason is that the rhombi pairs relax very rapidly to immobile squares and triangles. The diffusion process is strongly anisotropic and localized. The atoms move preferably through channels along the periodic axis. The anisotropy is much smaller than observed in Dzugutov's structure, however [24].

The triangular Z phase is the only crystalline phase where atomic jumps are observed. It is also the only case where diffusion without defects is possible in the solid state of the square-triangle system at $T^* = 0.6$. The tiles, however, do not change and the hexagonal structure remains intact. The atomic jumps are so frequent that it is even possible to observe long-range diffusion. Atoms move in all directions, but there is a small anisotropy: the diffusion in the stacking direction is slightly preferred. The reason for this behaviour is the following. The site at the center of the triangle is fifteen-fold coordinated and therefore rather big. The atom at this site is too small to fill this space, and can move so far away from its equilibrium position that an nearby atom may occupy its site. After this has happened, normal vacancy diffusion of edge or vertex atoms sets in. The vast majority of the jumps, however, still involve the central triangle atoms.

The Aper samples consist of a stacking of layers which are based on *different* tilings. These structures are therefore aperiodic also in the third direction. Since the different layers do not match perfectly with each other, we first have to relax the structure at $T^* = 0$. As only small shifts occur during relaxation, these structures can be called metastable. Even after relaxation there remain some mismatches, as can be seen in Figure 16 (left picture). At $T^* = 0.6$ a tiling without mismatches is formed, and periodicity is restored nearly everywhere during the simulation. This process lasts about 3000 time steps in the cubic Aper sample (and 16,000 time steps in the larger AperFlat samples, which will be discussed below). No untilable regions are left in the end, only point defects may be present. The behaviour of the atoms is different from the case without stacking disorder. In the beginning, the atoms move in plane to get to a low energy position. Then the atoms start to move, preferably along the periodic direction. In the Aper sample, only two places remain where the periodicity is broken at the end of the simulation.

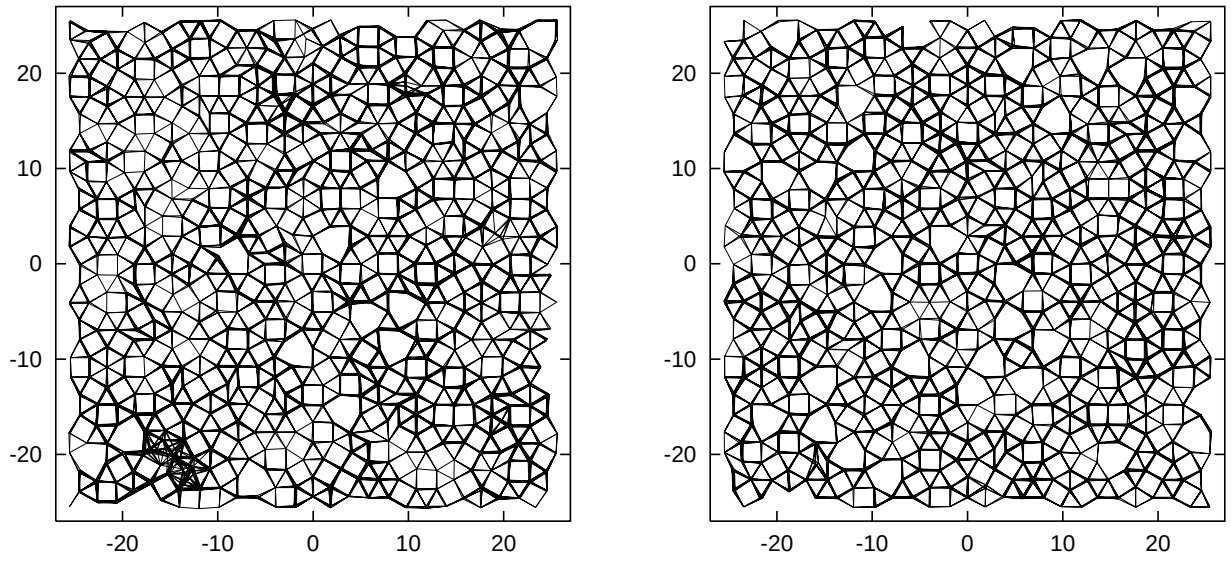

Fig. 16. Projection of the thermalized initial (left) and final (right) state of the tiling of the AperFlat sample, after 700,000 simulation steps. A comparison shows how the tiling has been reshuffled in many places. At the lower left corner of the left picture one can see that in the beginning of the simulation, there can be considerable mismatches between the tilings of the different layers. These are healed out during the simulation.

At these places the pattern in one layer is a shield, whereas in the neighbouring layer it is a cluster of a square, two triangles and a rhombus. The reason is that a half-vacancy has been created, which decouples the layers at this place. This configuration is stable through the whole 300,000 time steps simulated. The final structure of the Aper phase is a square-triangle-shield tiling like the Shi phase, but the distribution and frequency of the tiles is different from the Shi tiling.

This section can therefore be summarized as follows. In the phases where atom jumps occur at all (the Rho, Ran and Aper phases), we observe that changes in the structure occur at two levels: the tiling changes and the atoms move. The changes of the tiling can again be separated into several processes. If the stacking is imperfect, we have tiling reconstruction, and if there are rhombi we find tiling relaxation and tile flips. The tiling relaxation again consists of two parts, an immediate recombination of rhombi pairs and a slow transformation of single rhombi together with two squares and a triangle into a shield. The relaxation steps are reversible if the number of layers is small, in which case the single rhombi do not die out. The changes in the tiling are virtual moves, what really changes are the atom positions. We may again distinguish several processes. Atoms can jump from one place to another, travel a long distance, or hop forth and back between two states. Whereas the first two processes occur similarly in crystals, the last process is the materialization of the tile flips, which are highly correlated [31].

4.3 Flat samples without vacancies

In the flat samples we have only three layers instead of ten as in the cubic samples. This changes the behaviour completely. In contrast to the corresponding cubic Shi and SqTr samples, it is possible to observe flips in the flat ShiFlat and SqTrFlat samples. For the ShiFlat sample this happens already at $T^* = 0.6$. The initial number of shields increases until it is similar to the number found in the AperFlat structure. For the SqTrFlat sample we find that no tile transformations occur up to $T^* = 0.8$, but if the temperature is increased to $T^* = 0.9$, some shields are formed. This temperature is, however, extremely high compared to the melting temperature ($T^*_m = 0.95$), and it may happen that the sample is locally destroyed during simulation (depending on initial equilibration). This nevertheless corroborates our conclusion that the equilibrium state of our model is always of the square-triangle-shield type.

In the AperFlat sample flips are very frequent. Tiles flip forth and back, and all the basic flips described in Section 2.1 occur. We can even observe that the relaxation processes are reversed here and there. Frequent flips are in fact a general property of the flat samples. This is in contrast to the cubic samples with many layers, where flips are very infrequent and seem to die out completely after several hundred thousand time steps. No more than ten flips have been observed during 300,000 time steps in all the cubic samples together.

Pictures of the changes between the initial and final configurations of an AperFlat sample are presented in Figure 16. Only the tiles without the atoms have been drawn for clarity. A comparison of the structure before and after the simulation clearly shows the jumps of the tiles. The motion of the atoms during the simulations are revealed by Figure 17, where we have again connected the initial position of each atom with its final position. In the projection onto the quasiperiodic plane (left picture) one observes that the atoms move only very short distances, in most cases smaller than the nearest neighbour distance.

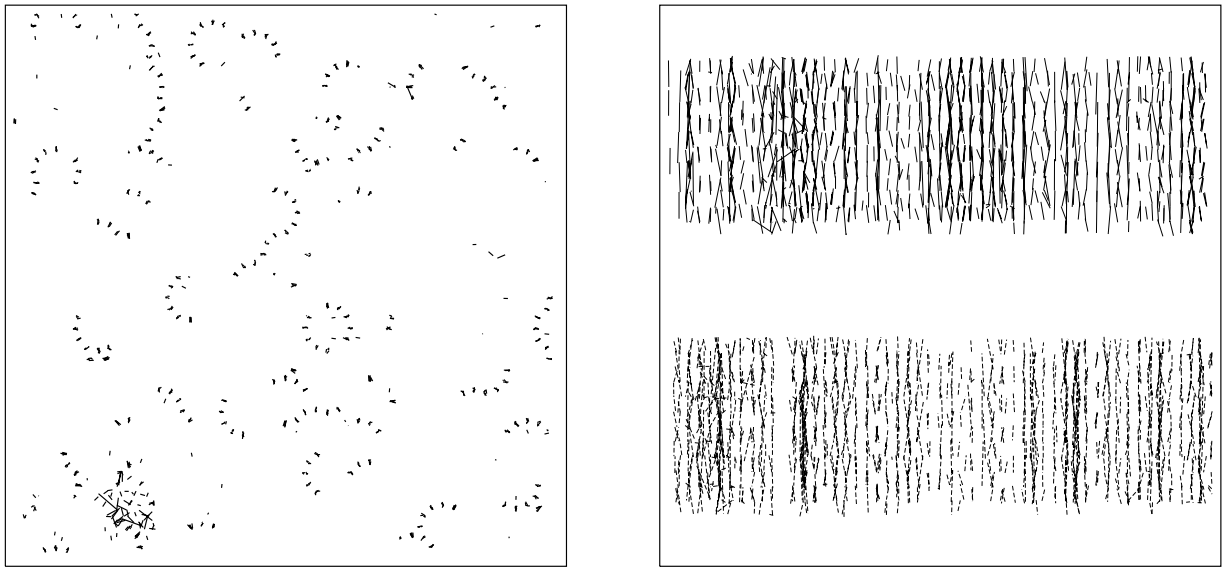

Fig. 17. Comparison of the initial and final configuration after 100,000 simulation steps, for the AperFlat sample. On the left, the projection on the quasiperiodic xy-plane is shown, with initial and final positions connected. On the right, projections on the xz- and yz-planes are shown, again with initial and final positions connected. One can clearly see that in the periodic direction atoms move much farther.

The projection onto a plane containing the periodic axis (right picture) shows that many atoms move long distances, similar to what we will find in the structures with vacancies.

To monitor the dynamics of the tile flips we have quenched the AperFlat sample every 1000 time steps. From the quenched configurations the tiling can then be recovered. The tiling does indeed change[3], as can be seen in Figure 18, where the trajectories of the tile centers are drawn. The moves of the atoms, however, can not be simply read off from the changes of the tiling. We therefore call these moves virtual. Most of the flips are rhombi-shield-rhombi (Fig. 4) and shield-rhombi-shield (Fig. 8) flips, only a few translational rhombi flips (Fig. 7) occur at the beginning of the simulation. Flip paths with up to four flips in different directions are found (Fig. 18). These flip paths show that tile flips propagate only very slowly, which is in agreement with the high correlation of flip diffusion found in Monte-Carlo simulations [31]. The atoms propagate even more slowly. In the quasiperiodic plane they do not get any farther than nearest neighbor distances in our simulation. This implies that atoms do not move together with the tiles. They travel much smaller distances. These results, which are obtained for *realistic* quasicrystal structures, show that one must be careful with the assumptions made in the Kalugin and Katz [1] model of diffusion in quasicrystals.

The behaviour of the AperFlat sample can be further quantified. The number of A-atoms n_A is directly related to the number of shields n_H and to the number of rhombi n_R. We have $n_R + n_A = a$ and $n_R = n_A - b$, with constants $a \approx 300$ and $b \approx 3600$ depending on the sample size. The number of A-atoms decreases sharply during about 60,000 simulation steps, due to the relaxation of rhombi pairs (see Fig. 19). The trend seems to continue during up to 700,000 steps, but simulations of the SqTrFlat and ShiFlat phases suggest that equilibrium should be reached soon after. The mean square displacement of the atoms shown in Figure 20 indicates two processes. The restoration of the tiling by jumps of the atoms in the quasiperiodic plane is achieved after about 200,000 time steps. On the other hand, the jumps along the periodic direction persist during the whole simulation. This observation

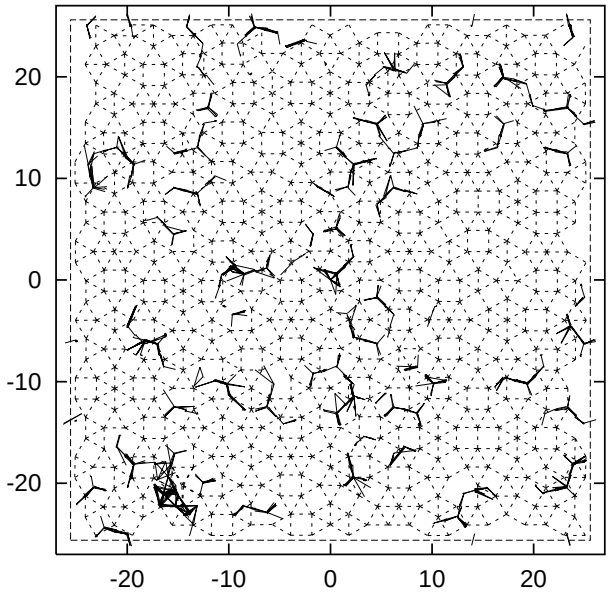

Fig. 18. Paths of the centers of the tiles.

[3] MPEG movies of the flipping tiles can be obtained by anonymous ftp at ftp.itap.physik.uni-stuttgart.de, in directory /pub/Film/.

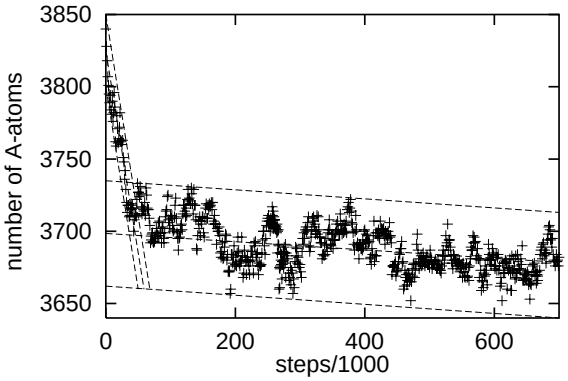

Fig. 19. Number of atoms in the A-Layer (AperFlat sample). The steep dashed lines indicate the initial relaxation process, the other dashed lines indicate that equilibrium has not yet been reached.

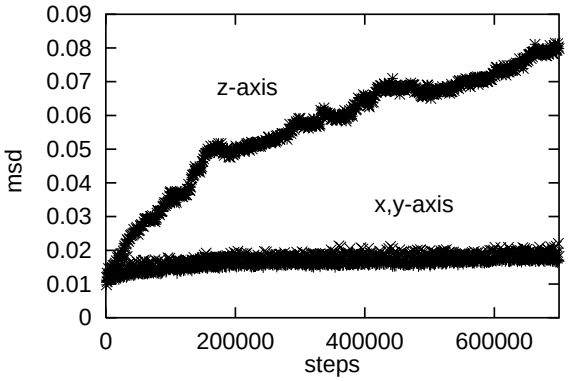

Fig. 20. Mean square displacements (msd) of the atoms along different coordinate directions (AperFlat sample).

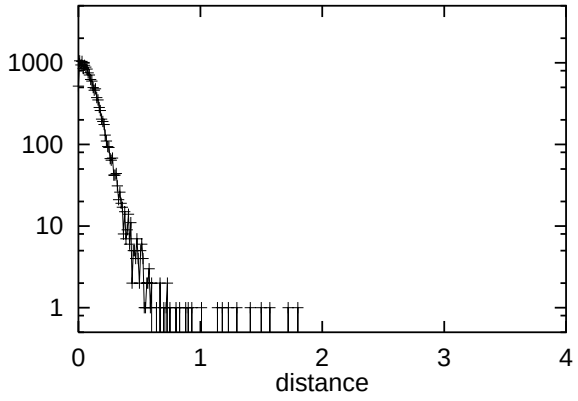

Fig. 21. Histogram of the displacements of the atoms along the x-direction after 700,000 steps (AperFlat sample).

is underlined by histograms of the distances by which the atoms travel during the simulation. Figure 21 shows that only a few atoms jump to a nearest neighbour site in the quasiperiodic plane, whereas Figure 22 indicates that the atoms jump consecutively from layer to layer along the periodic direction. Not all atoms take place in the jumps, but only atoms which happen to be at octahedral sites inside the shields.

In the flat samples, flips occur sufficiently often so that their frequency can be measured reliably. A jump

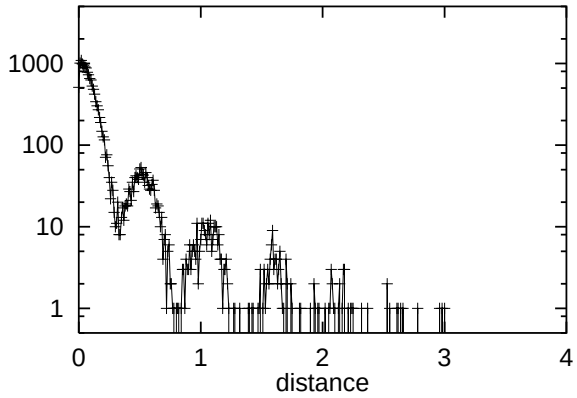

Fig. 22. Histogram of the displacements of the atoms along the z-direction after 700,000 steps (AperFlat sample).

of an atom chain along the periodic direction occurs every 110,750 time steps. The cosine of the angle between the directions of two successive jumps of the same atom is -0.169 on average, which means that successive jumps are nearly uncorrelated. A jump of a tile occurs about every 12,283 time steps, a jump of a rhombus every 21,123 and a jump of a shield every 29,288 steps. For rhombus-shield-rhombus flip the branching ratio between the backward and the two forward jumps is roughly 4:1:1, and for a shield-rhombus-shield jumps it is 13:4.

Extrapolating the results for the Rho, Ran and Aper phases for two different thicknesses to infinitely many layers, we are led to expect that *no flips* at all will be observed in an infinite sample. To further study the influence of the number of layers on the flip probability, we have used the Dod sample with a small cell size in the quasiperiodic plane, but with a varying number of periods. Figure 23 displays the resulting phase diagram, in which the transition temperature is shown as a function of the number of layers. Above this temperature, flips do occur during the first million time steps, but below they don't. Simulations with up to 3×10^8 time steps have been carried out for all possible tiling configurations in a dodecagon to make sure that a stationary state has been reached. This procedure is not possible for larger samples due to the large number of possible configurations and the increase of simulation time with sample size. The transition temperature increases nearly linearly with the number of layers, which indicates that for infinite thickness no flips occur below the melting temperature. In fact, already above about 12 to 13 $AB\bar{A}\bar{B}$ layers no flips are expected to occur any more.

4.4 Structures with vacancies

The simulations of the samples without vacancies prove that *in the absence of vacancies and half-vacancies* diffusion is possible only in samples with very few layers. In the thermodynamic limit, *i.e.*, with an increasing number of layers, the jumps and flips completely die out, due to a strong coupling along the periodic direction. In thermodynamic equilibrium, however, there is always an distribution of vacancies and half-vacancies present.

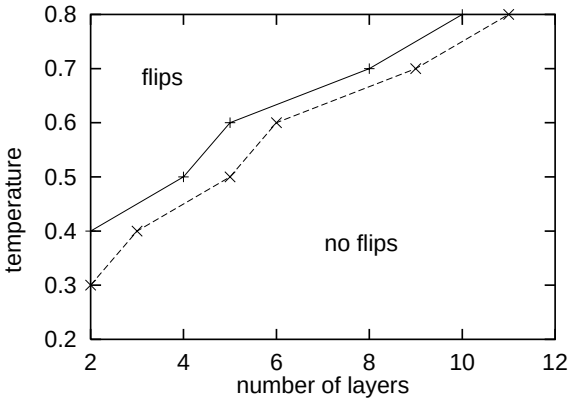

Fig. 23. Flip phase diagram for the Dod* models. The abscissa gives the number of periods, the ordinate the temperature. The two lines connect, respectively, the lowest temperatures where flips have occurred, and the highest temperatures where flips have not occurred during a simulation time of 1,000,000 steps.

Unfortunately, starting with a sample without vacancies this equilibrium distribution is difficult to reach. The same strong coupling in the periodic direction which hinders diffusion also hinders the formation of vacancies and half-vacancies. For this reason, we decided to introduce vacancies artificially, in a controlled way, either on specifically chosen classes of sites, or on randomly chosen sites, in oder to see how the equilibrium structure and the diffusion change in the presence of vacancies. Only the SqTr and Shi samples are used as starting configurations, because in these phases the atoms are the most immobile. A summary of the vacancy statistics is given in Table 3. These numbers show that vacancies are stable in the SqTr phase, but their number decreases in the Shi phase, which indicates that some vacancies are transformed into half-vacancies.

First we discuss vacancies in the SqTr phase. The different vacancy types (vert, edge, sq, tri) behave quite similarly. During 150,000 time steps we observe 23 to 35 nearest neighbour jumps along the periodic direction. In the SqTr_vert phase we also have a few consecutive jumps of the same atom. In the quasiperiodic plane there are only single jumps to nearest neighbor sites. The SqTr_any phase with different types of vacancies behaves a little differently. Only a total of 3 jumps along the periodic direction occur. The jumps are too infrequent for long-range diffusion to be observed reliably, although the mean square displacement of the atoms increases continuously during simulation. The fact that there are only nearest neighbour jumps indicates that it is normal vacancy diffusion what we observe.

We have also studied vacancies created inside the shields of the Shi phase. There are two types of such vacancies, ones that are analogous to the vacancies inside squares (Shi_sq phase), and ones that are at octahedral sites near the centre of the shield (Shi_oct phase). The behaviour of the Shi_sq phase is similar to that of the SqTr phase with vacancies. During 150,000 time steps, there are about 35 jumps to nearest neighbour sites, with an isotropic distribution. In the Shi_oct phase with 2.5% or 1.3% vacancies we find a different behaviour. Jumps to nearest neighbour sites are very frequent. The distances the atoms travel are 0.5 to 1 in the quasiperiodic plane, but up to 3 in the periodic direction (see Fig. 24), with all other integer multiples in between of the nearest neighbour distance (about 0.5) occurring too. This means that we see long range diffusion predominantly in the periodic direction, with atoms jumping from layer to layer. The jump distances indicate vacancy diffusion, although it is unusual that vacancy diffusion is so anisotropic.

The simulation results for the Shi_oct phase are displayed in Figure 25. If we compare the right picture with

Table 3. Number and type of vacancies for some of the samples: initial number of vacancies (I), number of vacancies after equilibration (E), final number of vacancies at the end of the simulation at $T = 0.6$ (F), and number of vacancies after additional quenching (Q).

phase	tot	I	E	EQ	F	FQ
Aper	8360	0	8	–	1	1
Ran	8360	0	0	0	0	2
NPT1	16384	404	365	370	442	427
NPT2	16770	91	31	33	99	83
NPT3	16888	74	19	21	82	76
NVT	16384	361	367	379	317	368
SqTr_any	8360	213	208	209	207	210
SqTr_edge	2840	210	210	210	210	210
SqTr_vert	2240	210	202	202	207	200
SqTr_squa	2080	235	210	210	211	210
SqTr_tri	1200	210	210	210	210	210
Shi_any	960	246	210	210	205	203
Shi_oct	960	209	195	182	193	183
Shi_oct (1.3%)	960	105	100	94	86	85

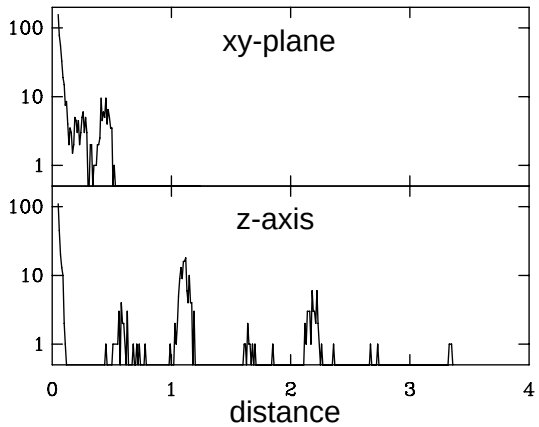

Fig. 24. Histograms of distances between initial and final atom positions after 100,000 simulation steps, for the Shi_oct phase containing about 2.5% vacancies. Distances both in the (periodic) z-direction and within the (quasiperiodic) xy-plane are shown. In the periodic direction, atoms get much farther, and there are clear, discrete step sizes. In the quasiperiodic direction, step sizes are much smaller, but there are still discrete step sizes apparent.

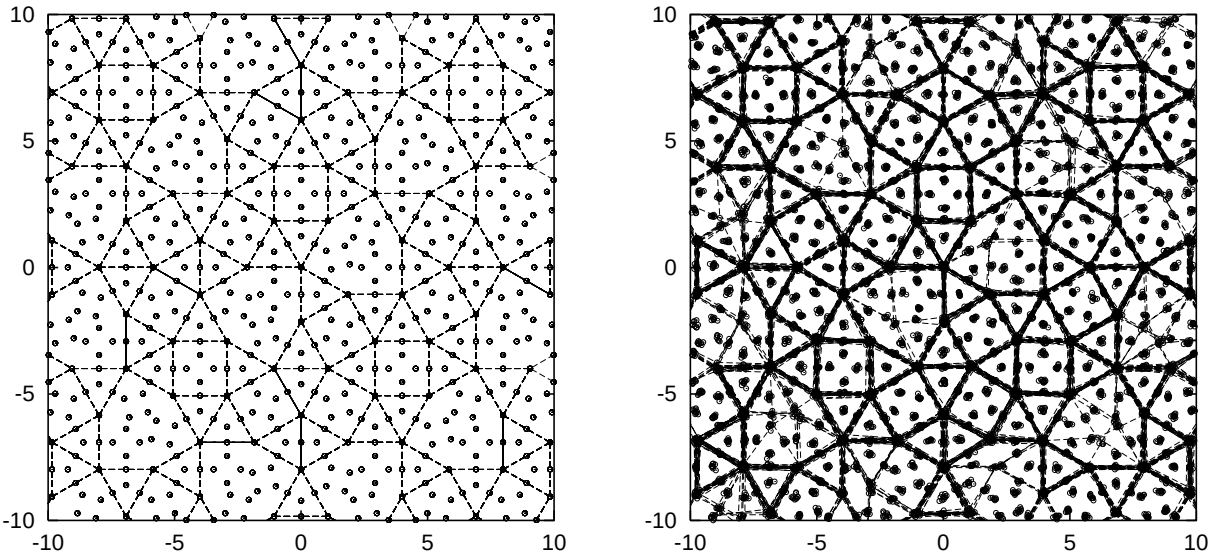

Fig. 25. Comparison of the initial and final configuration after 100,000 simulation steps, for the Shi_oct phase containing about 2.5% vacancies inside shields. On the left, a projection of the initial state on the xy-plane is shown. On the right, the same structure is shown at the end of the simulation. The tiling has been reshuffled, and at different z-coordinates one has different tilings, so periodicity is slightly broken. Atoms which have moved are primarily inside shields. The tile edges appear as heavy lines because the tilings at different z-levels, all drawn on top of each other, have been reconstructed from the thermally distorted atom positions.

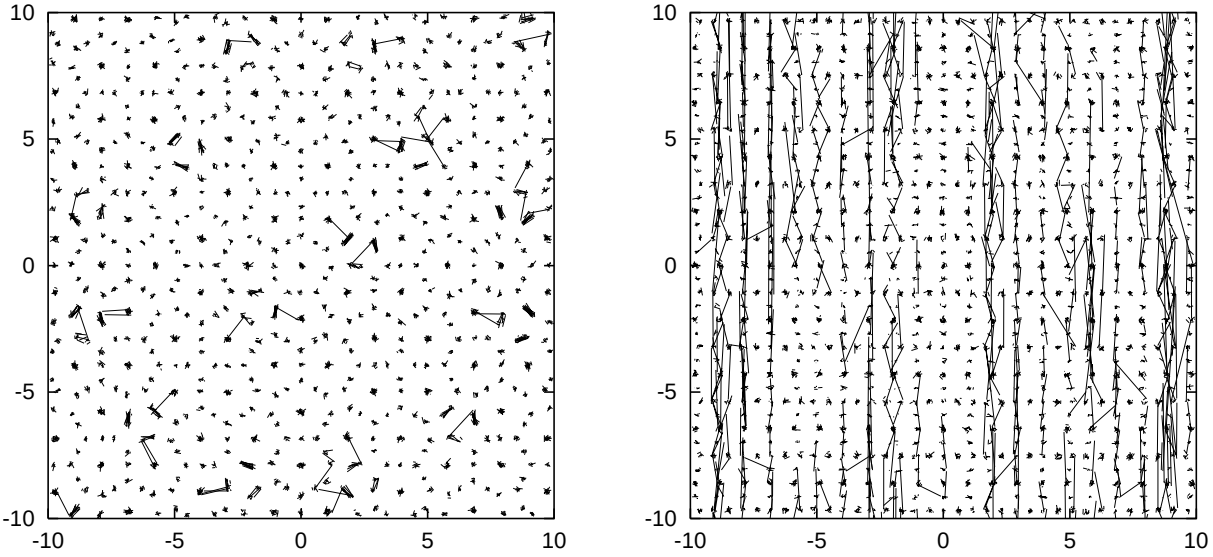

Fig. 26. Comparison of the initial and final configuration after 100,000 simulation steps, for the Shi_oct phase containing about 2.5% vacancies. On the left, a projection on the xy-plane is shown, with initial and final positions connected. On the right, a projection of the same structure onto the xz-plane is shown. It can be seen that atoms primarily move vertically, with small horizontal displacements only. Jumps of individual atoms are represented by straight line segments. Zig-zags of several line segments represent chains of atoms which follow each other. If a straight line extends over several layers (right picture), the corresponding atom must have performed several consecutive jumps.

the right picture of Figure 14, we find that we now have a large number of triplets of atoms. At these places the periodicity is broken, and half-vacancies are present. In Figure 26 (left picture) the shorter connecting lines represent the formation of triplets. In the right picture of Figure 26, it can been seen how far the atoms have moved along the periodic direction. In this case diffusion is strongly anisotropic.

Vacancies are most effective when they are created at octahedral sites inside the shields. The vacancies then catalyze the formation and elimination of rhombi inside shields. As expected, mobility is primarily in the periodic direction, whereas in the quasiperiodic plane atoms move only much shorter distances. We stress that in an infinite sample vacancies are necessary to allow columns of atoms to change their places at all. Vacancies therefore mediate

the flips and the flip diffusion in the quasiperiodic plane, besides leading to ordinary vacancy diffusion.

The atomic jumps in the presence of vacancies are different from those observed in simulations without vacancies. If there are no vacancies, the jump vector is often smaller than the atomic distance. The component along the periodic axis is half the interatomic distance, and the component in the quasiperiodic plane is even smaller. The correlation between two successive jumps is very high, the atoms often jump forth and back. This is in agreement with the high correlation of flips found in Monte-Carlo simulations [31]. Due to this high correlation, long range diffusion in the quasiperiodic plane is too slow to be observed in our simulations. If there are vacancies present, the jump vector is most frequently the average atomic distance, thereby indicating that we have predominantly ordinary vacancy diffusion. Since the tiling is reshuffled during the simulation, flip diffusion must be present too, but it is masked by the larger vacancy diffusion. The atoms often move long distances along the periodic direction, and sometimes also in the quasiperiodic plane. Successive jumps are much less correlated in the presence of vacancies.

4.5 Flip paths and activation energies

The trajectories of the atoms during an atomic jump or flip in a quasicrystal can be monitored using the molecular statics method as described, for example, by Beeler [32]. The method has to be adapted for our case, where not only single atoms jump, but a whole row of atoms changes its position. We first explain the procedure for the simplest case, the relaxation from two rhombi and a triangle to a triangle and a square. The flip is shown in Figure 2. We shall call the arrangement of the atoms in the rhombi-triangle version vertical (v), and the arrangement in the triangle-square configuration staggered (s). In the relaxation of two rhombi we have 2 atoms per period that move, which permits 6 degrees of freedom for the trajectory in three dimensions. Due to the mirror symmetry of the configuration, the degrees of freedom reduce to 4. It turns out that the distance of the atoms along the periodic direction remains constant and the center of mass of the jumping atoms projected onto the quasiperiodic plane remains unchanged. This removes 2 further degrees of freedom. The trajectory can well be approximated with a simple trigonometric function, and the only parameter which is left is the z-coordinate (or, equivalently, the orthogonal coordinate in the symmetry plane) of the flipping atoms.

The molecular statics calculation now works as follows. We start with the rhombi-triangle configuration surrounded by a typical shell of atoms. The flipping atoms are moved in small steps to new z positions, and after each step the configuration is relaxed by a potential energy optimization. In the relaxation the motion of the flipping atoms is restricted to the plane perpendicular to the periodic axis, for otherwise the atoms would move to the next minimum position. In this way it is possible to map the whole potential energy surface to find the extrema. From the potential energy surface one can determine both the flip path and the activation energy. For the rhombi-triangle-square flip (Fig. 2) we find that the original configuration is a maximum with an activation energy of 5.4 per period above the minimum.

The other flipping configurations, described in Section 2, permit up to three pairs of atoms per period to move. We have restricted the parameter space for each pair of atoms to the trajectories found in the rhombi-triangle case, but each pair may move independently of the other pairs. Inside a shield we have three pairs of atoms that can be moved (Fig. 5), whereas in the two-fold symmetric hexagon (Fig. 6) and in the translational shield flip (Fig. 8) there are two pairs.

The second configuration we shall examine is the twofold symmetric hexagon shown in Figure 6. The energy minimum is obtained for the sv-configuration in the middle of Figure 6. The ss-configuration at 1.4 per period is close to a saddle point with a small activation energy of 0.9 per period. At the saddle point the flipping atoms are shifted by 1/10 of the period along the z-axis. The saddle point also represents the energy barrier. The vv-configuration is a maximum at 5.3 per period. A typical flip of this configuration is given in Figure 7.

The most important configuration is the shield (Fig. 5). The energies per period are the following: the sss- and ssv-configurations are close together, the first being 0.35 per period above the minimum, and the second 0.60 per period. The real minimum is close to the ssv-configuration and is obtained by shifting the flipping atoms by 1/10 of the period along the periodic axis. The barrier between the sss configuration and the minimum is at 0.55 per period. The svv-configuration is a local maximum at 6.4 per period, and the vvv-configuration is a strong maximum at 17.5 per period. A typical flip is displayed in Figure 4. This flip is called the rhombus-shield-rhombus flip.

Finally, there exists a translational flip of the shield (see Fig. 8). It will be called the shield-rhombus-shield flip. The energy minimum is the vv-configuration, the sv-configuration is a local minimum at an energy of 0.3 per period, and the ss configuration exhibits a maximum at 5.5 per period. Between the vv and sv-configurations there is a barrier of height 0.5 per period above the minimum.

It seems strange, that for a single hexagon the minimum is the sss-configuration, but in the long shield the minimum is an vv-configuration. There may be two reasons for this. The first is that we have only considered limited clusters with one additional shell of atoms around the flipping tile configuration. Secondly, the potential energy surface in a dynamical simulation may be different from the statically determined one considered here. The long shield case, where more atoms are mobile, is closer to the dynamic treatment. One should also keep in mind that the (questionable) energy differences between the ss- and sv-configurations of the long shield, and between the sss- and ssv-configurations of the shield, are indeed very small compared with unfavourable configurations.

In summary, we find that pairs of rhombi are very unstable, single rhombi may easily change their position inside a shield by a rotational flip, or inside a twofold hexagon by a translational flip. Rhombi, together with squares and triangles, can also be transformed easily into a shield. Finally, a shield may change its position, if it has a neighbourhood as in Figure 8 ("long shield"). Such long shield configurations actually form a percolating cluster in a typical structure, so that long range tile diffusion should be possible.

4.6 Energies for vacancies and half-vacancies

We have calculated the energy cost for introducing vacancies and half-vacancies into the quasicrystal. For these calculations we have used a periodic approximant of edge length $3 + \sqrt{3}$ containing 180 atoms in a single period. This approximant has been chosen because it is the smallest one admitting two separated shields (due to geometric restriction there has to be an even number of shields and rhombi together).

The calculations were carried out with the molecular dynamics program with temperature and pressure set to 0.001 (for numerical stability reasons). A comparison with a constant volume simulation showed no significant difference in the average size of the simulation cell and the potential energies for the same number of periods. To compare samples with different numbers of periods per unit cell, however, the density of the simulation box had to be kept constant.

We first calculated the energies of a number of two-period perfect approximants (360 atoms) with shields and with one or both shields replaced by rhombi plus squares and triangles. Then we computed the energy of vacancies in an s column (in a shield) and in a v column (the shield replaced). There are two ways each to place the shields so that they have a) no common vertices (called separated), b) one common vertex (joined) or c) a common edge (fused). In total 16 samples without vacancies and 96 with a single vacancy can be constructed, but not all of these samples are different.

It would be too long to list all the results, so we will only sum up the trends here. The potential energy per atom of the tilings with two shields at different places already varies considerably (between -4.3744 and -4.3543), but the spectrum increases further if one or two of the shields are replaced (between -4.3935 and -4.3503). On average, the energies per atom with one or two rhombi are lower than for the tiling they have been constructed from, but there are also examples where the energy with shields is as low as with rhombi. For the sake of completeness we also mention the energy of a pure square-triangle configuration: -4.39008.

It turns out that the energy of a vacancy is largely independent of the sample. It varies between 6 and 7.2. For this reason, we could confine a detailed study of the vacancy energies to one representative sample. A vacancy in a vertical chain (6.72) is slightly more favourable than in a staggered chain (6.82). The average coordination number is 13.667, and since only nearest neighbour interactions are present, the binding energy of one atom has about the same value. This means that the energy cost of one vacancy is quite small.

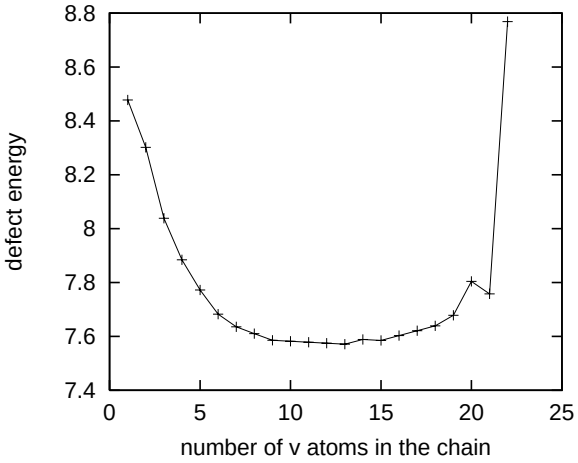

Fig. 27. Energy of half-vacancies for a sample with 12 periods, as a function of vertical atoms. The energy as a function of staggered atoms is obtained if the x-axis is inverted.

After it was clear that the vacancy energy is largely independent of the particular tiling, we chose one sample with a fixed rhombus and a shield, into which the staggered/vertical chain with half-vacancies could be built in. For this tiling we calculated the potential energies per atom for the shield and the rhombus configuration, for two up to ten periods ($E_{pot} = -4.37942$ and -4.38238, respectively). It turns out that the energies are completely independent of the number of periods (if the volume is fixed).

Next we computed the vacancy energies for two up to ten layers. With increasing number of layers, the vacancy energies decrease from 6.12 to 5.92 for the v configuration, and from 6.49 to 6.32 for the s configuration. The vacancy energy is proportional to the reciprocal number of layers. The limit is obtained at about 5 to 6 layers.

For vacancies only their mutual distance is relevant. On the other hand, half-vacancies always occur in pairs, due to the periodic boundary conditions, so their energy depends on the number of periods (size of the sample), but also on the distance between the two parts of a pair. Due to the periodic boundary conditions a chain with half-vacancies always contains a segment with staggered (s) atoms and a segment with vertical (v) atoms. To calculate the half-vacancy energies, we have to subtract the weighted total potential energy of the perfect samples with the vertical and staggered configuration from the total potential energy of the sample with the half-vacancies. The weight was chosen according to the number of atoms in the staggered and vertical configuration. The smallest possible distance between the two half-vacancies is 3/4 of a period. In this case, only one atom separates the two parts of the vacancy. This configuration is only (meta-)stable if the separating atom is at a vertical position. Otherwise the half-vacancy parts collapse into a vacancy.

The result for a half-vacancy pair with $n_p = 12$ periods is shown in Figure 27. The figure displays the energy as a function of the number of vertical atoms n_v. The energy as a function of the staggered atoms is obtained by replacing n_v by $n_s = 2*n_p-1-n_v = 23-n_v$. The energy decreases with increasing distance between the parts of the defect pair. The last point is the defect with only one s atom, which is unstable as noted above. The plateau in the middle of the plot shrinks if the number of periods is reduced.

The results can be summarized as follows. Fused shields cost more energy than joined shields, and these in turn cost more energy than separated shields. Shields cost more energy than rhombi. Vacancies in rhombi (vertical chain) cost less energy than in shields (staggered configuration). The vacancy energy decreases with the number of periods. Half-vacancy pairs again cost more energy than vacancies. The energy of a half-vacancy pair decreases if the two parts move apart and the atoms in between are in the vertical configuration. If the atoms between are in the staggered configuration, close half-vacancies are instable, and the energy remains approximately constant if the distance between the two parts is increased. For all the defects encountered, the energy is between 2/3 and 1/2 of the energy that the breaking of the bonds to nearest neighbours would cost.

All the calculations have been carried out for the low temperature quasistatic case. At finite temperature, the small differences between the different tilings and configurations will be washed out by the vibrations of the atoms. The kinetic energy will also help the atoms to split a vacancy into two half-vacancies and to change from the rhombus to the shield configuration. In addition, the shields and rhombi are usually much farther apart from one another, and this may also change the energetical behaviour, as can be seen in Section 4.5, where the chain flips have been discussed.

5 Discussion and conclusions

In our MD simulations we have investigated the different diffusion mechanisms that occur in the dodecagonal quasicrystal system. Apart from ordinary vacancy diffusion, we have also observed a diffusion mechanism which is specific to layered, 1-periodic quasicrystals. In this mechanism, the atoms jump from A-type layers to B- and $\bar{B}$-type layers, and *vice versa*, thereby transforming vertical chains of atoms to staggered ones, and *vice versa*. Such flips change the tiling in the quasiperiodic plane, but they propagate only very slowly. The flips of the tiling appear to be highly correlated, which is actually not too surprising, in view of the results of reference [31]. In the same way, the atoms hardly propagate in the quasiperiodic plane, but only hop forth and back most of the time. This new diffusion process will be called chain hopping since, eventually, entire chains have to hop in order to produce diffusion in the quasiperiodic plane. This process is therefore rather different from the mechanism proposed by Kalugin and Katz [1] and used in many Monte-Carlo simulations of flip diffusion.

The geometry of the structure changes in the chain hopping process is quite complicated. The jump distances of atoms in the quasiperiodic plane are much shorter than the virtual distances by which the tile centers move. This is quite similar to the decagonal Zeger-model [33], where the flips of two pairs of atom chains virtually change the position of huge clusters, thereby pretending a tiling change on a much larger scale.

Chain hopping and vacancy diffusion are not independent. Vacancies and half-vacancies catalyze the flips, especially in infinite samples where whole infinite columns have to be moved. This is achieved by breaking the perfect periodicity during simulation, which is possible at higher temperatures due to atom vibrations and lattice expansion with temperature. We find that a sizable density of half-vacancies and vacancies is always present in equilibrium, which is necessary to make chain hopping possible at all. Without their presence, there would be no diffusion. We should emphasize, however, that the flip mechanism, although catalyzed by vacancies, is qualitatively different from vacancy diffusion, in that the passage of a vacancy without flips associated with it leaves the structure unchanged, whereas with the flips the structure is left completely reshuffled after the passage of the vacancy.

The diffusion in our model is anisotropic, and can be subdivided into two components at least. We recall that half-vacancies or vacancies are involved in all diffusion processes we have observed. Vacancies lead, on the one hand, to ordinary vacancy diffusion, which is isotropic. On the other hand, vacancies and half-vacancies can also catalyze flips, which produce diffusion in all directions too, but this diffusion component is much smaller in the quasiperiodic plane than in the periodic direction. The small shifts in the quasiperiodic plane and the half integer jumps in the periodic direction are due to the flip diffusion, whereas the integer jumps in all directions result from ordinary vacancy diffusion. In the quasiperiodic direction the vacancy part is the dominant one, whereas in the periodic direction both components contribute.

5.1 Quasicrystals with other symmetries

Our model quasicrystals are somewhat untypical in that they are periodic in one direction. This causes problems because flips have to break periodicity to be feasible, and thus lead to larger mismatches. Icosahedral Frank-Kasper-type quasicrystals based on the Henley-Elser model [34] are quite similar to the dodecagonal quasicrystals, but do allow for flips which are purely local. They need, however, at least two types of atoms to be stable. Simulations have shown that it is not possible to exchange atoms of different type without destroying the structure. The chain hopping process is replaced by a monoatomic ring processes involving five or ten atoms at special sites in the neighbourhood of dodecahedra and oblate rhombohedra. These tiles are the counterpart to the rhombus and shield in the dodecagonal case.

The model structures used in this work are mostly tetrahedrally close-packed, which makes them very rigid. Stable quasicrystals like AlPdMn and AlCuFe are not so densely packed. They contain empty octahedral interstitial positions. Some models [35–37] predict that they are based on pseudo-Mackay-clusters with a highly mobile inner shell. This may change the diffusion behaviour profoundly.

5.2 Related results of Dzugutov

The stability of the Frank-Kasper-type decoration of the square-triangle-rhombi-shield tiling was discovered by Dzugutov [17]. Dzugutov's goal was to produce a monoatomic glass from the melt by rapid quenching. He used the special potential discussed in Section 13 to disfavour simple crystalline structures, which would usually nucleate. After cooling below the glass transition temperature he found a glass which, after a very long annealing time, is transformed into a dodecagonal quasicrystal. The underlying tiling structure is mainly a decorated square-triangle tiling with a few rhombi and shields. This is exactly the structure which appeared in the SqTrFlat, ShiFlat and AperFlat simulations to be the most stable (Sect. 4.3). For the cubic samples the same statement can not be made, since we could not reach equilibrium due to the less frequent jumping of the longer chains.

In the structure found by Dzugutov, the quasiperiodic plane is not parallel to a coordinate axis as in our simulations (Sect. 2), but has an arbitrary orientation. This implies that a walk perpendicular to the plane does not close after one circuit, but has a certain offset. It further leads to a frustration of the tiling: after one circuit the tiling is shifted relative to the initial tiling, but since it is aperiodic, there are mismatches which can not be eliminated and lead to ongoing flips in the simulation. In contrast to our Rho, Ran, Aper samples (Sect. 4.2), the flipping activity will therefore not stop after a certain time, since there is no unique minimal configuration.

Dzugutov [24] observed up to 2.5% vacancies, which he regards as a generic feature of the structure. We think, however, that this may not be true, since he cools at constant volume [25], which may force the system to create vacancies to compensate the shrinking average atomic distance. He also does not distinguish vacancies and half-vacancies. The latter occur predominantly at places where the tiling changes from layer to layer.

Dzugutov's structure also contains a two-dimensional extended defect with a width of two to three interatomic distances, cutting through the quasiperiodic layers. Flips occur primarily along the defect, thereby shifting its position. This defect represents a stacking fault connected with a partial screw dislocation with a Burgers vector of 1/4 of the AA-layer distance in the periodic direction. A further consequence is, that the layers are not perfectly flat, but twisted. This planar defect is another source of half-vacancies and vacancies.

The atomic jumps and phason flips observed by Dzugutov [24] are exactly the ones introduced in Section 2, which are observed also in our simulations. Dzugutov claims that the flips require defects like vacancies, since in a dense packing of atoms it is not so easy to shift atoms locally. Our simulations basically confirm this: even though flips are possible without vacancies in systems with only few layers, the number of flips rapidly decreases to zero if the number of layers is increased. In samples with few layers, the thermal expansion of the lattice allows the creation of half-vacancies, which in turn can break the periodicity and catalyze the tile flips. With an increasing number of layers, however, it becomes harder and and harder to reach an equilibrium density of vacancies in a MD simulation, so that the tile flips are suppressed if vacancies are not introduced artificially. In the case of Dzugutov's sample, the persistent stacking frustration and lacking periodicity clearly help to maintain a sufficient number of defects to catalize the flips.

Dzugutov [24] further finds a very high diffusion rate and a small anisotropy. The diffusion along the periodic direction is larger than in the quasiperiodic plane. Particles in the defective region are much more mobile than in the bulk. He claims that there are at least two different diffusion processes: conventional vacancy jumps and the phason hopping. We think that it is necessary to add a further component in his case: there is also grain boundary diffusion involved, due to the planar defect. In our simulations we find that vacancy diffusion on most sites is indeed fairly isotropic (Sect. 4.4). There is, however, the strongly anisotropic component of vacancy and half-vacancy diffusion on octahedral sites. To test the influence of the vacancies on the diffusion, we have filled them in Dzugutov's structure, but the diffusion constant decreases only by a factor of 1.5 to 2.5, depending on the number of filled-in atoms. The vacancies even reappear after long simulation runs, and the volume increases a little, to adjust the density for the additional atoms. This result shows, that the effect of the additional imperfections are not negligible and cannot be quantified. This was one of our main reasons to choose perfect tilings for our simulations, and to introduce defects in a controlled way.

5.3 Related theoretical results

Our simulations of a realistic, layered, three-dimensional dodecagonal quasicrystal indicate that flip diffusion and similar processes may be much more complicated than described in the paper of Kalugin and Katz [1]. In contrast to the simple theory, atoms are not only located at the vertices of the tiling, but the tiles are decorated in a complicated way, which means that a lot of atoms take part in one flip. Flips could involve additional tiles not present in the ground state. The jump distance of the atoms may be much shorter than the flip of the tiling vertices.

The predictions of Kalugin and Katz [1] have been tested by a number of groups [2,4,5,3,6,7] in Monte-Carlo simulations for pure tiling models, without taking into account any a specific atomic decoration of the tilings. While such an approach proves that elementary flip processes do add up to diffusive behaviour, the physical feasibility

of the flip mechanism and the magnitude of flip diffusion remain much less certain. In particular, activation energies of elementary flips cannot be estimated without a specific atomic structure and a definite atomic interaction. It is also not clear at which temperatures flip diffusion may be relevant.

Oxborrow and Henley [23] have studied the two-dimensional undecorated dodecagonal square-triangle tiling in detail. They show that simple local flips like the ones permitted in a rhombus tiling are not possible. To change the tiling, one has to create flippable configurations in form of a pair of rhombi, and then flip a whole sequence of tiles, until the rhombi recombine again. This move has been called a zipper. Our simulations have shown, that the creation of flippable configurations is a quite natural process, since it is easily possible to create rhombi and shields (Sect. 4.3). It may even be possible to have a ground state which already includes shields.

5.4 Related experimental results

Joulaud *et al.* [12,13], Zumkley *et al.* [14,15] and Sprengel *et al.* [16,38] find that self-diffusion and hetero-diffusion in quasicrystalline AlPdMn and AlCuFe above $T \approx 600\,^{\circ}\mathrm{C}$ is similar to what is known from similar crystalline Al alloy phases. The diffusion follows an Arrhenius law, and the activation energy as well as the pre-factor can be explained easily by vacancy diffusion. Measurements by Blüher *et al.* [39] indicate that there is a significant change in the diffusion parameters at low temperatures for Pd and Au diffusion in AlPdMn. This behaviour is not known for crystals, but has some similarity with what is known for amorphous structures. It is speculated that this is the contribution of the quasicrystal-specific flip diffusion.

Coddens *et al.* [8–10] and Lyonnard *et al.* [11] have observed atomic jumps directly in AlCuFe and AlPdMn, using inelastic neutron scattering and Mößbauer measurements. With quasi-elastic neutron scattering they observe Cu jumps in AlCuFe with a distance of 4 Å (size of the elementary clusters), and possibly also jumps with a distance of 2.7 Å. Since the temperature independent width of the signal is $\Gamma = 55\ \mu$eV, the process is too fast to be ordinary diffusion. The intensity follows an Arrhenius law with an activation energy of $Q = 755$ meV, which means that it is an assisted process, possibly by Al vacancies. The observation is explained by assisted phason hopping. It can not be explained by cluster vibrations and collective modes. The Mößbauer results yield a jump vector of 2.5 Å for Fe, with a width of $\Gamma = 4\ \mu$eV. De Aráujo *et al.* [40] conclude from the time dependent second order Doppler shift and the anomaly of the Debye-Waller factor in Mößbauer spectroscopy that they do not observe lattice vibrations, but Fe hopping. The intensity of the scattering signal is constant with Q, while the width scales with ΔQ^2. This behaviour is opposite to what is expected from the theory of Kalugin and Katz [1].

The long jump vectors observed by Coddens and Lyonnard [41] are distances between second neighbours. The less frequent shorter jump vectors connect nearest neighbours. This result is quite different form ours: the jump vector component in the quasiperiodic plane is about 1/4 of the atomic distance, the component along the periodic axis is 1/2. The distance for vacancy jump processes, however, is the atomic distance. The coupling we observe between vacancies and half-vacancies on the one hand, and flips on the other hand, clearly shows that the jump processes we observe are assisted processes.

The authors would like to thank to M. Dzugutov for making available the structure obtained in his simulation, and C. Beeli for suggesting the atomic flip moves. This work was started during a stay of both authors at the Laboratory of Atomic and Solid State Physics at Cornell University, where it was supported by DOE grant DE-FG02-89ER-45405 and Packard Foundation grant FDN 89-1606. The major part of the simulations were done on computing facilities generously provided by the Cornell Materials Science Center. The first author was supported by Deutsche Forschungsgemeinschaft, the second author by the Swiss Nationalfonds and the Swiss Bundesamt für Bildung und Wissenschaft in the framework of the HCM programme of the European Community.

References

1. P.A. Kalugin, A. Katz, Europhys. Lett. **21**, 921 (1993).
2. D. Joseph, M. Baake, P. Kramer, H.-R. Trebin, Europhys. Lett. **27**, 451 (1994).
3. M.V. Jarić, E. Sørensen, Phys. Rev. Lett. **73**, 2464 (1994).
4. D. Joseph, F. Gähler, in *Aperiodic'94*, edited by G. Chapuis and W. Paciorek (World Scientific, Singapore, 1995), pp. 188–192.
5. F. Gähler, in *Proceedings of the 5th International Conference on Quasicrystals*, edited by C. Janot and R. Mosseri (World Scientific, Singapore, 1995), pp. 235–239.
6. M.V. Jarić, S.L. Johnson, E. Sørensen, in *Proceedings of the 5th International Conference on Quasicrystals*, edited by C. Janot and R. Mosseri (World Scientific, Singapore, 1995), pp. 363–366.
7. W. Ebinger, J. Roth, H.-R. Trebin, Phys. Rev. B **58**, 8338 (1998).
8. G. Coddens, R. Bellissent, Y. Calvayrac, J.P. Ambroise, Europhys. Lett. **16**, 271 (1991).
9. G. Coddens, C. Soustelle, R. Bellissent, Y. Calvayrac, Europhys. Lett. **23**, 33 (1993).
10. G. Coddens, S. Lyonnard, B. Sepiol, Y. Calvayrac, Evidence for atomic hopping of Fe in perfectly icosahedral AlCuFe quasicrystals by ^{57}Fe Mößbauer spectroscopy. preprint.
11. S. Lyonnard, G. Coddens, Y. Calvayrac, D. Gratias, Phys. Rev. B **53**, 3150 (1996).
12. J.L. Joulaud, C. Bergman, J. Bernardini, P. Gas, J.M. Dubois, Y. Calvayrac, D. Gratias, J. Phys. IV Colloq. France **6**, 259 (1996).
13. J.L. Joulaud, C. Bergman, J. Bernardini, P. Gas, J.M. Dubois, Y. Calvayrac, D. Gratias, Phil. Mag. A **75**, 1287 (1997).

14. T. Zumkley, H. Mehrer, K. Freitag, M. Wollgarten, N. Tamura, K. Urban, Phys. Rev. B **54**, R6815 (1996).
15. T. Zumkley, M. Wollgarten, M. Feuerbacher, M. Freitag, H. Mehrer, in *Diffusion in Material, Part 1*, edited by H. Mehrer, C. Herzig, N.A. Stolwijk, H. Bracht, Defect and Diffusion Forum (Scitec Publications, Uetikon, 1997), Vol. 143-147, pp. 843-848.
16. W. Sprengel, T.A. Lograsso, H. Nakajima, in *Diffusion in Materials, Part 1*, edited by H. Mehrer, C. Herzig, N.A. Stolwijk, H. Bracht, Defect and Diffusion Forum (Scitec Publications, Uetikon, 1997), Vol. 143-147, pp. 849-854.
17. M. Dzugutov, Phys. Rev. Lett. **70**, 2924 (1993).
18. F. Gähler, in *Quasicrystalline Materials*, edited by C. Janot and J. M. Dubois (World Scientific, Singapore, 1988), pp. 272–284.
19. C. Beeli, F. Gähler, H.-U. Nissen, P. Stadelmann, J. Phys. France **51**, 661 (1990).
20. F. Gähler, J. Roth, in *Aperiodic'94*, edited by G. Chapuis and W. Paciorek (World Scientific, Singapore, 1995), pp. 183–187.
21. T. Ishimasa, H.-U. Nissen, Y. Fukano, Phil. Mag. A **58**, 835 (1988).
22. M. Conrad, *Tantalreiche Telluride*, Ph.D. thesis, Dortmund, Germany, 1997.
23. M. Oxborrow, C.L. Henley, Phys. Rev. B **48**, 6966 (1993).
24. M. Dzugutov, Europhys. Lett. **31**, 95 (1995).
25. M. Dzugutov, Phys. Rev. A **46**, R2984 (1992).
26. M.P. Allen, D.J. Tildesley, *Computer Simulations of Liquids*, (Oxford Science Publications, 1987).
27. D.J. Evans, G.P. Morriss, Chem. Phys. **77**, 63 (1983).
28. V.N. Kabadi, W.A. Steele, Molec. Simul. **4**, 371 (1990).
29. A.V. Chadwick, in *Defects and Disorder in Crystalline and Amorphous Solids*, edited by C.R.A. Catlow, (Kluwer Academic Publishers, 1994), pp. 25–48.
30. J. Roth, *The phase diagram of the Dzugutov potential*, in preparation.
31. F. Gähler, A. Hirning, *A correlated random walk model for phason-assisted diffusion*, in preparation.
32. J.R. Beeler, *Radiation Effects Computer Experiments* (North Holland, Amsterdam, 1983).
33. G. Zeger, H.-R. Trebin Phys. Rev. B **54**, R720 (1996).
34. C.L. Henley, V. Elser, Phil. Mag. B **53**, L59 (1986).
35. C. Janot, Phys. Rev. B **53**, 181 (1996).
36. V. Elser, Phil. Mag. B **73**, 641 (1996).
37. A. Katz, D. Gratias, J. Non-Cryst. Sol. **153-154**, 187 (1993).
38. W. Sprengel, T.A. Lograsso, H. Nakajima, Phys. Rev. Lett. **77**, 5233 (1996).
39. R. Blüher, P. Scharwaechter, W. Frank, Phys. Rev. Lett. **80**, 1014 (1998).
40. J.H. de Aráujo, A.A. Gomes, J.B.M. da Cunha, Sol. State Commun. **97**, 1025 (1996).
41. G. Coddens, S. Lyonnard, Physica B **226**, 28 (1996).